L-A-64

# CANADA - NWT

# MINERAL DEVELOPMENT AGREEMENT

Giant Yellowknife Mines Limited
Yellowknife Division
Recovery Improvement Project

Volume 2



Canada

Northwest Territories Canada

Canada-NWT

Mineral Development Agreement

Northern Technology Assistance Program

# Giant Yellowknife Mines Limited
# Yellowknife Division
# Recovery Improvement Project

Volume 2

---

No. SC-265237

March 1990

Prepared by: S.L. Chryssoulis
Process Mineralogy
Surface Science Western Ontario
The University of Western Ontario

CANMET Scientific Authority:

M.J. Stefanski
Physical Scientist

GIANT YELLOWKNIFE MINES LIMITED
Yellowknife Division

Recovery Improvement Project
#SC-265237

Phase II

VOLUME 2

March 1990

# PROCESS MINERALOGICAL STUDY OF Au IN CONCENTRATOR AND CALCINE SAMPLES FROM GIANT YELLOWKNIFE, N.W.T.

For: GIANT YELLOWKNIFE MINES LTD.
MILL DEPARTMENT
P.O. BOX 3000
YELLOWKNIFE, N.W.T.
X1A 2M2

Attn: Mr. G. Halverston, P.Eng.
Mill Superintendent

by

PROCESS MINERALOGY
SURFACE SCIENCE WESTERN
THE UNIVERSITY OF WESTERN ONTARIO
LONDON, ONTARIO
N6A 5B7

Prepared by:
S.L. Chryssoulis

SSW/PMS/90/1

## LIST OF CONTENTS

## LIST OF TABLES

## LIST OF FIGURES

## LIST OF PLATES

## LIST OF APPENDICES

## SUMMARY

A detailed study of the process mineralogy of gold in samples from the flotation circuit and the roaster and cyanidation plants was conducted, in order to identify possibilities for improving the gold recovery in the GIANT Yellowknife metallurgical plant.

The following techniques were used: **optical microscopy** (to characterize the native gold, in terms of size and association); **diagnostic cyanidation** (to determine the native gold fraction); **scanning electron microscopy with EDX** (to determine the composition of the native gold, and characterize the calcine particles in terms of porosity and permeability, **ion probe microanalysis** (to quantify the submicroscopic gold concentration within the sulphide and oxide minerals); and **ion imaging** (to determine the submicroscopic gold distribution within individual mineral particles). **Submicroscopic gold** is solid solution gold in the sulphide crystal structure and colloidal gold (< 0.1 $\mu$m) within sulphides or oxides. Mineralogical balances for gold were obtained by combining normative and modal analysis data with results of the above techniques.

**Arsenopyrite** is the **principal gold-carrier mineral** in the GIANT Yellowknife ore. The submicroscopic or 'invisible' gold within arsenopyrite accounts for 59.7% (normalized to 100) of the assayed gold in the classifier o/f. The average submicroscopic gold concentration of 105 arsenopyrite particles is 299 **ppm**. The **submicroscopic gold** is **inhomogeneously distributed** and areas of high gold content are located in the outer zones of the arsenopyrite grains.

Native Au has 6.9 wt% Ag and accounts for 38.7% of the assayed gold in the classifier o/f. The liberated coarse-grained native Au accounts for 67.5% of the cyanidable Au, and floats readily in the Maxwell cell concentrates and the rougher concentrate. Of the remaining native Au 10.3% is associated with quartz, 9.8% with pyrite and 12.4% with arsenopyrite. Of the unliberated gold 23.0% is combined with sulphides and 45.2% is locked within sulphides (Figure 1). The unliberated gold with pyrite and coarse-grained arsenopyrite is recovered in the Maxwell cell concentrates and rougher concentrate.

The fine-grained arsenopyrite is enriched in submicroscopic gold (495 ppm) relative to the coarser grained arsenopyrite (153 ppm). The fine-grained arsenopyrite is the principal gold carrier in the scavenger concentrate accounting for 75.7% of the assayed gold. Fine-grained arsenopyrite is the principal gold carrier in the 'low' grade tailings (0.014 oz/T) and accounts for the refractory to direct cyanidation gold in the 'high' grade tailings (0.021 oz/T). The additional gold in the 'high' grade tailings is native Au relatively coarse combined with quartz. This is cyanidable without regrind. The gold mineralogical distribution in the flotation tailings and concentrates is given in Figures 2 and 3.

Gold losses in the flotation circuit can be minimized by recovering the coarser native Au that is associated with quartz and floating more of the fine-grained gold-rich arsenopyrite.

In the **roaster calcine** the **gold is colloidal.** Gold in maghemite particles is not readily amenable to cyanidation because of the limited number of relatively coarse pores running parallel to the rim of the particle which do not contribute to a pervasive permeability. Gold in the goethite/hematite/scorodite mixed particles is readily amenable to cyanidation because of the pervasive permeability offered by numerous multidirectional micropores. Sintered impermeable coatings reduce permeability and therefore gold recovery, but this can be corrected by regrinding. The peripheral distribution of the gold enriched areas in arsenopyrite particles represents a favorable configuration because the colloidal gold is leached easier. However, if the rim becomes impermeable the colloidal gold within the rim becomes locked and is not recovered even by regrinding.

TABLE 1 - GOLD MINERALOGICAL DISTRIBUTION, %

(not normalized)

| SAMPLE | CYANIDABLE | SUBMICROSCOPIC AU IN ARSENOPYRITE | SUBMICROSCOPIC AU IN PYRITE | TOTAL |
|---|---|---|---|---|
| classifier o/f | 41.2 | 63.6 | 1.7 | 106.5 |
| 'high' grade tails | 52.2 | 74.8 | 2.1 | 129.1 |
| 'low' grade tails | 50.0 | 81.3 | 2.3 | 133.6 |
| 1st Max. cell conc. | 35.0 | 58.9 | 2.2 | 96.1 |
| 2nd Max. cell conc. | 36.0 | 50.9 | 2.5 | 89.4 |
| Rougher concentrate | 29.0 | 65.1 | 1.3 | 95.4 |
| Scavenger concentrate | 25.0 | 81.5 | 1.1 | 107.6 |

## 1.0 INTRODUCTION

In this report are presented results of the mineralogical study on the distribution of Au in selected GIANT Yellowknife samples. This investigation is part of a major effort to improve the Au recovery from 87% to +90%. The samples to be studied and the objectives of the mineralogical investigation were set during two meetings. In the first meeting on 30/3/89 participated Mr. G. Halverston, mill superintendent; Mr. B. Starcheski, mill engineer of GIANT Yellowknife Mines and S. Chryssoulis of Surface Science Western. The second meeting was in Yellowknife on 18/4/89 between B. Starcheski and S. Chryssoulis when sampling details were discussed. Finally on 20/10/89 the interested parties met to discuss the progress of investigation and results. The objectives of the study were the following:

1. To identify the sulphide mineral(s) in which the submicroscopic gold is concentrated, and quantify the Au by ion probe microanalysis;
2. To obtain a complete mineralogical balance for gold in a representative sample of the classifier overflow, and samples of a 'low' and a 'high' grade tailings;
3. To determine the process mineralogy of Au in the concentrator by studying concentrate samples;
4. To determine the principal Ag carrier minerals in the classifier overflow, in order to evaluate the possibility of using Ag as an indicator for electrum;
5. To identify the phases in the calcine, prior and after cyanidation which carry the Au, and to determine their submicroscopic Au concentration by ion probe microanalysis;

6. To obtain images of the submicroscopic Au distribution in oxidized sulphide and sulpharsenide particles and to correlate with porosity where possible.

The scope of this process mineralogical study is to fully characterize the occurrence of gold in the ore mill and roaster products, in order to identify ways to improve the recovery, and assist the mineral processor in organizing the appropriate set of laboratory tests.

**Submicroscopic** Au is defined as solid solution and colloidal Au (1-0.001 $\mu$m) in the crystal lattice of minerals.

All the objectives set at the onset of the investigation were addressed successfully in this study.

## 1.1 SAMPLING

The following concentrator and roaster samples were provided for chemical assaying and Au process mineralogical investigations:

#1 classifier o/f, as is;

#5 classifier o/f - 200 mesh cyanided;

#8 high grade tailings, as is;

#11 low grade tailings, as is;

#14 roaster calcine, as is;

#15 calcine residue, as is;

#16 calcine, pulverized and CN leached;

#18 1st Maxwell cell concentrate;

#19 2nd Maxwell cell concentrate;

#20 Rougher concentrate;

#21 Scavenger concentrate.

In total 8 samples from the flotation circuit, and 3 from the roaster and leaching circuits were examined in terms of their Au mineralogy, using methods discussed in the next section.

## 2.0 METHODOLOGY

The approach used to determine the Au process mineralogy involved chemical assaying, diagnostic cyanidation, sizing and density separations, optical microscopy, scanning electron microscopy with X-ray analysis, ion probe microanalysis for Au and As, and ion imaging for Au, As, S and Fe.

### 2.1 SAMPLE PREPARATION

At the concentrator site two 500 g sub-samples were separated from each sample for diagnostic cyanidation testing.

Sub-samples for chemical assaying were separated from all samples as received. The classifier o/f samples (#1 and #5) and the tailings samples (#8 and #11) were sieved. The +200 mesh size fraction was separated into a heavy and a light fraction using a sodium metatungstate aqueous solution with a density of 2.8 - 2.9 g. $cm^{-3}$. Both density fractions were assayed. The -200

mesh size fraction was cyclosized and the slime fraction (< ~ 20 $\mu$m) obtained by combining the product in cones 4 and 5 with the cyclosizer discharge were assayed.

The roaster calcine (#14), calcine residue (#15), and the releached calcine residue (#16) samples were sized using the 200 mesh sieve. The same sizing and cyclosizing, was used with the four concentrate samples (#18-#21). The coarse fraction of the calcine and the calcine residues samples were separated by density or using a strong hand magnet. Results on sizing and density separations are given in Appendix A1.

Sizing was used to prepare better polished sections for studying under the optical microscope and to maximize the number of coarser particles per section suitable for ion probe microanalysis. For the same reason the +200 mesh size fractions were either separating by density or magnetically, that is for concentrating the sulphide or iron oxide fractions. For modal analysis polished mounts from unseparated samples were used. In total 68 polished mounts were prepared and examined by one or more of the methods discussed in the following sections.

## 2.2 OPTICAL MICROSCOPY

The following tasks were addressed using reflected light microscopy: to determine the ore minerals in the flotation samples; to select and mark sulphide particles suitable for ion probe microanalysis; to determine the characteristics of the gold minerals; to determine the oxide mineralogy and

texture in the calcine samples, and to select and mark oxide particles for ion probe microanalysis. The determination of the processing characteristics of the gold minerals, the modal analysis, and the particle selection were done at 800X magnification. The other tasks were addressed at 320X. Photographic 'maps' of the marked sections were taken using a microscope to facilitate locating the particles to be analyzed by the ion microprobe or SEM.

## 2.3 SCANNING ELECTRON MICROSCOPY

An ISI-DS 130 Scanning electron microscope (SEM) equipped with a energy dispersive x-ray analyzer (EDX) was used to analyze the gold minerals, to verify the composition of some sulphides and examine to the porosity of the calcinated particles. Typically, magnifications from 1500X to 3000X were used. The composition of the gold minerals was determined using the standardless quantification program of Tracor Northern. By using electrum grains that had been analyzed previously on an electron microprobe by EDX and quantified using metal standards, it was determined that the accuracy of the standardless quantification was satisfactory (±15% for Ag). The analyses were done at 20 KeV.

## 2.4 ION PROBE MICROANALYSIS

An upgraded CAMECA IMS-3f secondary ion mass spectrometer (SIMS) or ion microprobe was used for the determination of the submicroscopic Au within the sulphide and oxide minerals. The ion probe is the ideal instrument for detecting and quantifying the submicroscopic Au concentration in single mineral grains because of its superior sensitivity, the spot size and depth

profiling capabilities. It is 1000 times more sensitive than the electron probe (under normal operating conditions) and 100 times more sensitive than the proton microprobe or $\mu$-PIXE. The minimum detection limit, MDL ($3\sigma$), for Au in pyrite is 0.28 ppm with an analysis area of 60 $\mu$m in diameter. The depth profiling capability of the ion microprobe, which is not available with other microprobe techniques, allows the detection and differentiation of hidden sub-micrometer inclusions. A typical example is shown in Figure 4. The depth profiling capability of the ion probe is the result of the destructive nature of this technique, with successively deeped atomic layers being removed and analyzed with time (Figure 5).

The procedure for SIMS analysis involves the localization of a marked particle under the optical microscope attached to the instrument with the aid of the photographic map, and the placement of the particle in the path of the primary beam. The centering of the particle with respect to the beam is ensured by viewing the crater produced (optical microscope) and by monitoring the ion image of a major isotope in the mineral analysed (fluorescent screen). Thus for pyrite the $^{34}S$ image is used, for arsenopyrite $^{75}As$ and for the iron oxides $^{56}Fe$. The primary beam is rastered to ensure that a flat bottomed crater is produced and that there are no edge effects; a requirement for the Au implanted oxides. The primary beam was used in the spot mode when the sample had not been implanted (external standardization). In both cases a 60 $\mu$m area was analyzed. A smaller analysis area, 25 $\mu$m, is used with very small grains, but with loss in sensitivity. With a 60 $\mu$m analysis area the minimum detection limit ($3\sigma$ of background signal) for Au in pyrite is 0.28 ppm, in

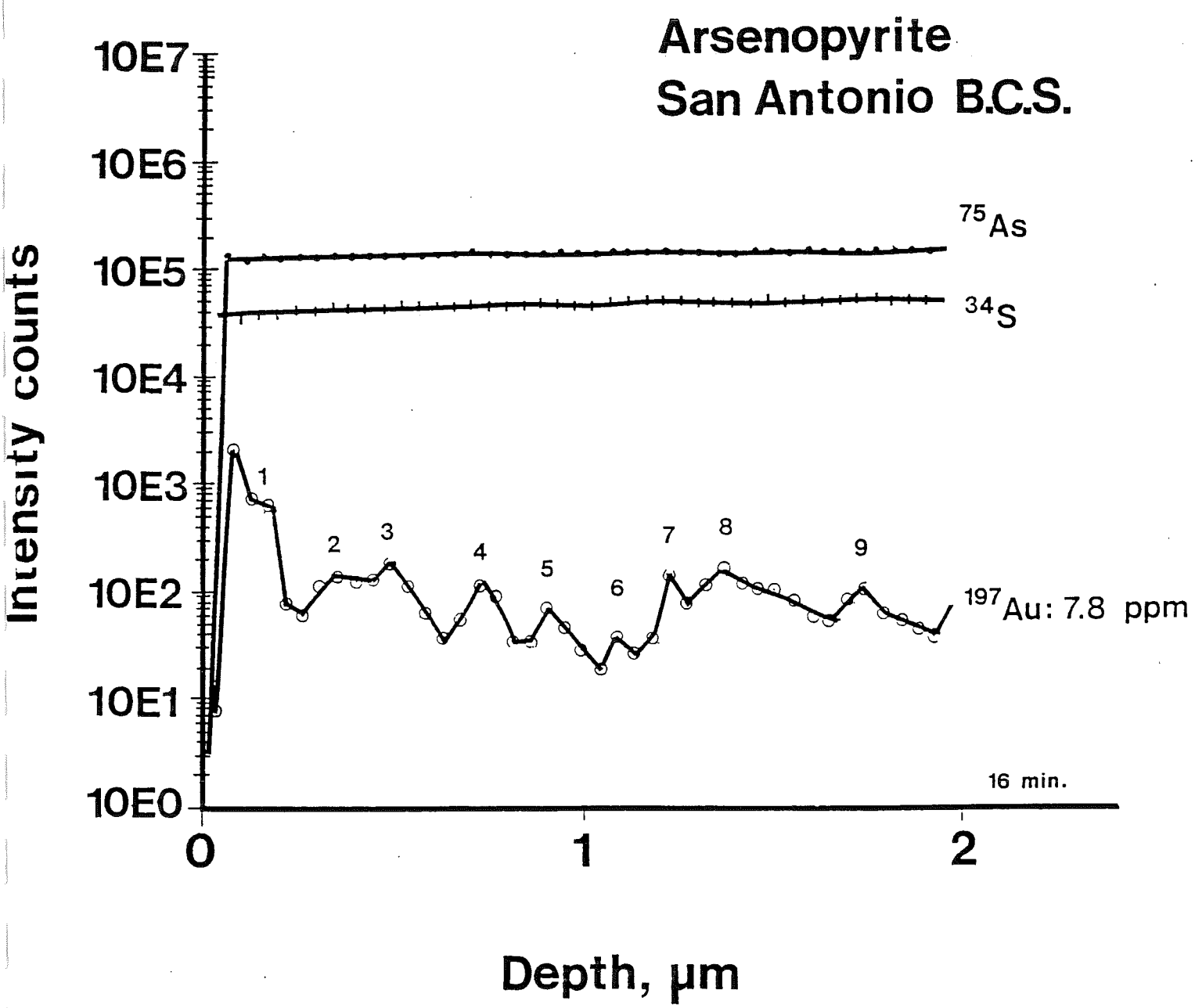


FIGURE 4 - 'Hidden' sub-micrometer Au inclusion in arsenopyrite

arsenopyrite 0.20 ppm and in maghemite 0.10 ppm. With the 25 $\mu$m analysis area the MDL is 1 ppm. The operating conditions are given in Table 2. A schematic diagram of the instrument is given in Figure 6. Details on the sample preparation and standardization procedures can be found in Cook and Chryssoulis, (1990); Chryssoulis et al., (1987) and Chryssoulis (1989).

Gold has only one isotope, the $^{197}Au^-$. Isobaric molecular interferences from $^{197}CsS_2^-$, $^{197}FeAsS_2^-$ and $^{197}Si_2O_7^-$ were eliminated by voltage offsetting as discussed by Chryssoulis (1989).

**External standardization** (Chryssoulis et al., 1989) by means of calibration curves was used to quantify the submicroscopic Au concentration in the Giant Yellowknife pyrite and arsenopyrite. The precision of the external standardization was determined to be 20% from the scatter of the standard data points about the least square calibration line. Ion implanted pyrite and arsenopyrite grains were used as external standards as discussed by Chryssoulis (1989).

**Internal standardization** by means of ion implantation was used to quantify the submicroscopic Au concentration in the calcine mineral phases. Since the analyzed calcine particles are smaller than the area rastered by the primary beam, the measurement of the depth of the crater produced had to be done on large (>300 $\mu$m) particles. Thus the sputtering rate for each 'type' of calcine particle found in the GIANT Yellowknife roaster calcine and calcine residue was determined and used in the equation for internally

**TABLE 2 - OPERATING CONDITIONS**

| | |
|---|---|
| Beam: | $Cs^+$ |
| Current: | 400 - 500 nA |
| Voltage offset: | 150V (quantitative analysis)<br>100 V (imaging) |
| Energy offset: | 50 eV |
| Rastered area: | 250 x 250 $\mu$m |
| Spot size: | 50 - 70 $\mu$m |
| Analysis area: | 60 $\mu$m diameter circle |
| Analysis time: | 4 - 8 min. |
| Depth of analysis: | < 1 $\mu$m (sulphides)<br>< 2 $\mu$m (oxides) |
| Standardization: | external (sulphides)<br>internal (oxides) |
| Minimum Detection Limit: | 0.28 ppm (pyrite)<br>0.20 ppm (arsenopyrite)<br>0.10 ppm (maghemite) |

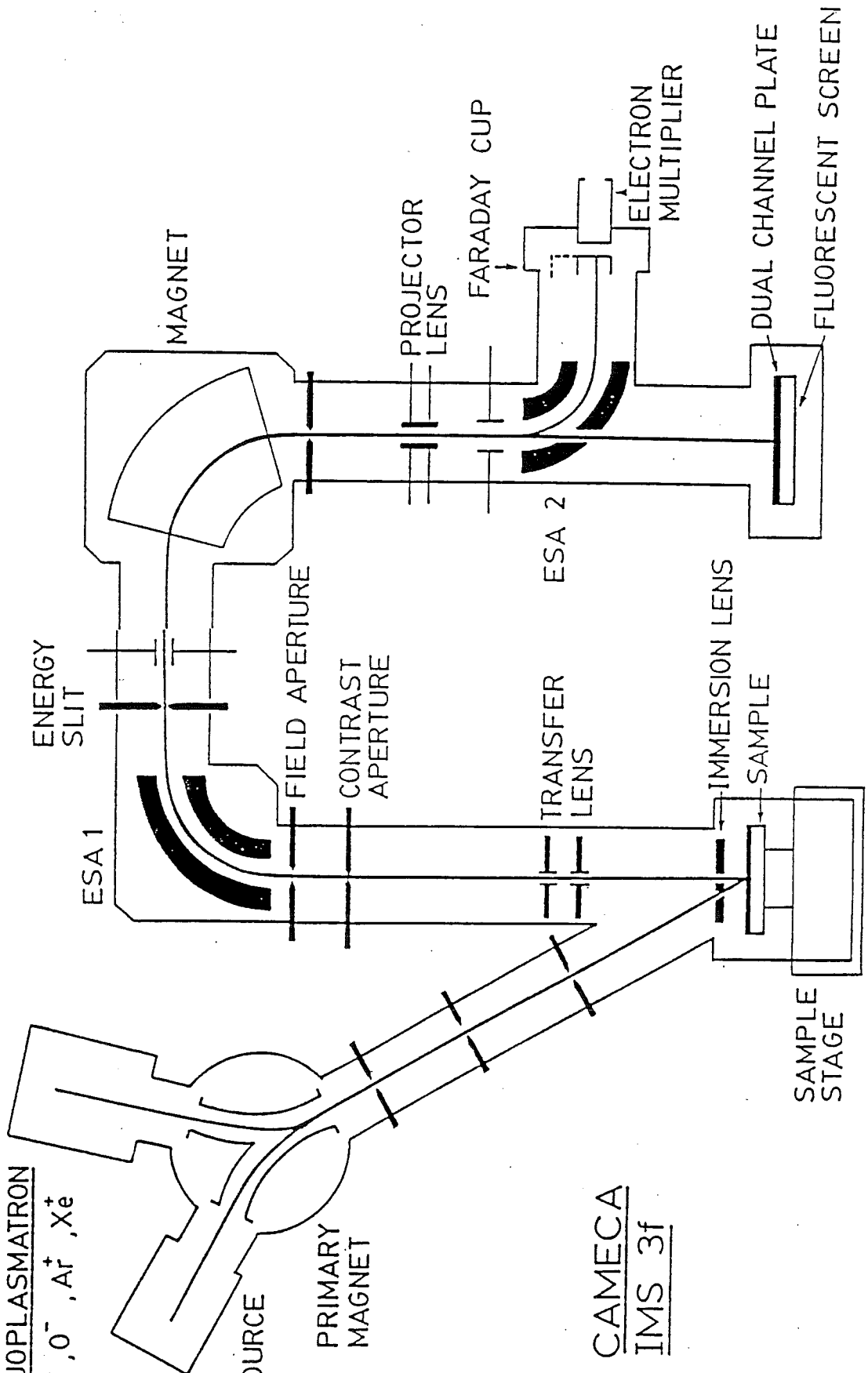


FIGURE 6 - Schematic diagram of the ion microprobe

standardized samples (Chryssoulis et al., 1987):

$$Co = \frac{F \,.\, Io \,.\, 197}{r.\ t.\ Ii \,.\, N.\ d} \times 10^{-2} \text{ (ppm)}$$

where:

Co = Au concentration in particle (ppm)

F = implant dose (Au, atoms $cm^{-2}$)

Io = integrated signal from original submicroscopic Au in the particle

Ii = integrated signal from implanted Au in the particle

t = time of analysis (s)

N = Avogadro number ($6.022 \times 10^{23}$ atoms $mol^{-1}$)

r = sputtering rate ($22 Å s^{-1}$ for maghemite, $47 Å s^{-1}$ for goethite/ scorodite)

d = density of particle ($g.\ cm^{-3}$)

The estimated precision of the internal standardization as applied in the GIANT Yellowknife calcine samples is 20% - 25%. The worse than normal (15%) precision is due to (i) the inhomogeneous nature of the particles analyzed, which frequently are composed typically of two closely intergrown mineral phases, and (ii) small variations, 5 - 10% in the sputtering rate from particle to particle.

The **accuracy** of the ion probe microanalysis for Au in sulphide minerals was determined to be better than 13% at the one part per million concentration level (Chryssoulis et al., 1987).

To summarize, the **precision of an individual determination of submicroscopic Au in a GIANT Yellowknife sulphide particle is 20%.** For example if the particle assayed 20 ppm Au, the random error (precision) is ±4 ppm. **The precision of an individual determination of submicroscopic Au in a calcine particle is better than 20%.** For example if the particle assayed 10 ppm Au, the random error is ± 3 ppm. The precision of an individual determination as discussed here should not be confused with the **confidence interval ($\lambda$) of the average submicroscopic Au content** in a given mineral. The confidence interval ($\lambda$), is a measure of the expected variation of the average Au content, as the result of the statistical variation of the Au content within individual particles of that mineral. The confidence interval of the average is determined at the 95% significance level, that is if the same number of grains were analyzed 100 times, in 95 the average will be within the prescribed range.

Recently, a limit of detection of 10 ppm for Au in pyrite was achieved with the electron probe (Graham, 1988) by using a high current 500 nA (normal ~ 20 nA) and accelerating voltage, 40 KeV (normal 15 - 25 KeV). Under these operating conditions mineral grains from processing circuits cannot be analyzed because of sample degradation and increase in the volume of microanalysis. A further complication may arise from the presence of micrometer size hidden Au mineral inclusions in the grains analyzed. The analysis time (not reported) is expected to be approximately 10 to 20 minutes, limiting the number of grains which can be analyzed per day to 30% of those analyzed with the ion probe (60).

## 2.5 GOLD MINERALOGICAL DISTRIBUTION

The mineralogical distribution of gold together with the characteristics of the gold carrier minerals (physical association and size distribution) are valuable information to the metallurgist involved in process design or optimization.

In order to determine the mineralogical distribution of gold the following information is required:

(i) direct or calculated Au head assay,

(ii) gold concentration in each Au-carrier mineral, and

(iii) concentration of each Au-carrier mineral.

The calculated head assay from cyanidation tests, in the absence of cyanicides and preg-robbing carbon, is the best estimate of the Au head assay, since the sample size is larger (500 or 1,000 g. versus 30 g.)

The gold concentration in the gold minerals (native Au, electrum) was determined by electron probe microanalysis, while the submicroscopic gold concentration in pyrite and arsenopyrite was measured with the ion microprobe.

Image analysis or normative analysis was used to determine the concentration of the Au-carrier minerals. **Normative analysis** is the term used to describe the calculation of mineral contents from chemical assays. Image analysis (or point counting) was used for determining the relative abundance

of different types of a sulphide, for example fine- and coarse-grained arsenopyrite that may have different invisible Au contents. Image analysis was useful also when the ore had sulphides of similar composition, for example pyrite, pyrrhotite, marcasite.

The GIANT Yellowknife ore has two major sulphides: pyrite and arsenopyrite. The other sulphide minerals combined account for less than 2 wt% of the ore. Since arsenopyrite is the only arsenic mineral, as a first approximation all arsenic was assigned to arsenopyrite using the stoichiometric formula FeAsS. The unallocated to arsenopyrite sulphur is used to calculate the pyrite ($FeS_2$) concentration. Since pyrite has arsenic in minor concentrations, and is present in significant amount in the GIANT Yellowknife concentrates a better estimate of the sulphide mineral concentration was obtained by determining the amount of arsenic in the pyrite (from the pyrite content and the ion probe data on arsenic in pyrite) and using the unallocated As to determine a new concentration for the arsenopyrite and pyrite.

The precision of the normative determination is a function of the precision of the chemical assays and the true arsenic and sulphur content of the GIANT Yellowknife arsenopyrite and pyrite.

## 2.6 GOLD ION IMAGING

The CAMECA IMS-3f ion microprobe has been used to produce ion images of the submicroscopic gold distribution in sulphide and oxide minerals. In the

case of the sulphides these images are important because they depict clearly (i) the degree of concentration of the submicroscopic gold, (ii) the association with other elements (As) and (iii) the size and location of areas having high gold contents within the sulphide particles. Such information is useful for the selective treatment of the gold-rich areas in pyrite, minimizing the time and the cost of processing as well as environmental contamination. In the case of oxides the images identify areas in the particle which contain the unleached gold, thus enabling the determination of the factors that resulted in the formation of the unleached gold.

The diameter of the ion images is 150 $\mu$m. The interfering moleculars are eliminated by 100V offsetting with a 50 eV wide energy window. The image produced on the fluorescent screen is transferred to an Everex 1800 computer using a CCD video camera. The camera is cooled to minimize circuit noise, appearing on the images as vertical lines. The images are stored in the computer memory or on floppy disks for processing and to obtain hard copies (transparencies or photographs).

For major isotopes ($^{34}S$, $^{56}Fe$, $^{75}As$) the number of frames required ranges from 50 to 400 depending on the mineral, image intensity and uniformity of the signal. For minor and trace elements ($^{75}As$, $^{197}Au$) the number of frames required ranges from 500 to 2,000 because of the lower signal. Typically, an averaging routine is used with the brighter images, while a summing routine is employed for low intensity images. The estimated minimum detection limit for imaging submicroscopic gold in pyrite is approx-

imately 20 ppm. However in metallic matrices, gold concentrations as low as 0.84 ppm have been imaged (Chryssoulis and Weisener, 1989).

## 3.0 RESULTS

### 3.1 CHEMICAL ASSAYS

The samples were assayed for Au, Fe, As and S. The analyses were done both at the mine site and Lakefield Research to ensure reproducible results and estimate the accuracy. All assays are given in Appendix A2. In Tables 3 - 5 are the assays used for the mineralogical distribution of Au.

The direct Au assay of the classifier overflow ranges from 8.57 g/t (0.25 oz/T) to 10.1 g/t, and the average direct Au assay is 8.89 ± 0.61 g/t.

The 'high' grade tails average direct Au assay is 0.72 ± 0.09 g/t (3 assays), and the 'low' grade tails average is 0.27 ± 0.21 g/t (3 assays). The significantly larger confidence interval of the average Au assay in the 'low' tails is due to the low Au assays from Lakefield 0.21 and 0.13 g/t compared to 0.48 from the mine site laboratory. For the mineralogical balances of gold in the tailings samples the assays from the mine site were used i.e. 'high' tails 0.72 g/t Au and 'low' tails 0.48 g/t Au because they are considered to be more representative (Table 3).

The gold assays of the concentrates from the mine site laboratory and Lakefield Research are very close. Thus the 1st Maxwell cell concentrate assays 109.3 ± 1.4 g/t Au, the 2nd Maxwell cell concentrate 113.5 ± 7.0 g/t

TABLE 4 - ARSENIC ASSAYS (wt%)

| SAMPLE | GIANT Y. | LAKEFIELD R. | $\hat{x} \pm \lambda$ |
|---|---|---|---|
| classifier o/f | .88,.89,.88 | 0.92, 1.10 | 0.93 ± 0.08<br>0.89 ± 0.02 |
| 'high' tails | 0.087 | 0.086, 0.080 | 0.084 ± 0.004 |
| 'low' tails | **0.062** | 0.081, 0.073 | 0.072 ± 0.011 |
| Maxwell 1 conc. | 11.04 | 12.7 | 11.9 ± 1.7 |
| Maxwell 2 conc. | 10.73 | 12.2 | 11.5 ± 1.5 |
| Rougher concentrate | 8.79 | 10.1 | 9.5 ± 1.3 |
| Scavenger concentrate | 3.04 | 3.0 | 3.02 ± 0.04 |

IN BOLD ARE FIGURES USED IN THE Au MINERALOGICAL BALANCE

TABLE 5 - SULPHUR ASSAYS (wt%)

| SAMPLE | GIANT Y. | LAKEFIELD R. | $\hat{x} \pm \lambda$ |
|---|---|---|---|
| classifier o/f | 2.2,2.04,2.53 | 2.03, 1.98 | 2.16 ± 0.20<br>2.06 ± 0.10 |
| 'high' tails | 0.25,0.24,0.23 | 0.16, 0.14 | 0.20 ± 0.05 |
| 'low' tails | 0.27,0.15,0.15 | 0.16, 0.12 | 0.17 ± 0.05<br>0.15 ± 0.02 |
| Maxwell 1 conc. | 27.48 | 32.1 | 29.8 ± 4.6 |
| Maxwell 2 conc. | 31.98 | 37.0 | 34.4 ± 5.0 |
| Rougher concentrate | 15.27 | 16.1 | 15.7 ± 0.8 |
| Scavenger concentrate | 5.37 | 3.94 | 4.7 ± 1.4 |

IN BOLD ARE FIGURES USED IN THE Au MINERALOGICAL BALANCE

Au, the rougher concentrate 81.9 ± 0.7 g/t Au and the scavenger concentrate 27.1 ± 2.7 g/t Au. Thus the larger error is in the assay of the scavenger concentrate, 10% (Table 3).

The arsenic assays are given in Table 4. The arsenic assays from Lakefield were consistently higher than those from the mine site laboratory. The confidence intervals of the average As assays range between 1 and 15%. The maximum compounded random error in the calculation of the arsenopyrite content in these samples will be 16% and the average precision for all samples 11%.

The sulphur assays are given in Table 5. In samples with low sulphur content there is good agreement between the two laboratories, and the average sulphur assays (minus outsiders) were used in the normative calculations. In the Maxwell concentrate samples the sulphur assays from the mine site are consistently low and the Lakefield assays were used. This is because the Lakefield high sulphur assays have been checked with other laboratories and found to be acceptable (Chryssoulis, 1987). The sulphur for the rougher concentrate samples are comparable and the average sulphur was used, as with the scavenger concentrate. The maximum compounded random error in the calculation of the pyrite content in the samples will be 25% in the 'high' tails sample. However it has little effect on the Au mineralogical balance because both the pyrite content and the 'invisible' gold concentration in the pyrite are low. In the Maxwell 1 and 2 concentrates the random error in the estimation of the pyrite content will be 15%.

## 3.2 DIAGNOSTIC CYANIDATION

Direct cyanidation tests were performed at the mine site, using 500 g. charges of the classifier o/f, the 'high' and 'low' grade tails, the concentrate and the roaster calcine samples. Results are given in Table 6. These tests were done using rolling bottles for 48 h. at pH10 with 2 g NaCN/l.

Three samples of the classifier o/f were ground to different degrees in order to determine the effect of grinding upon recovery. The gold recovery increased only marginally from 41.0% to 41.8% by increasing the fineness of the grind from -200 mesh to -325 mesh. Assuming that free cyanide was available, the cyanidation tests indicate the presence of refractory gold, which can be either locked fine-grained Au, or submicroscopic Au in the pyrite and arsenopyrite. An average recovery of 41.2% was used in the classifier o/f Au mineralogical balance.

Cyanidation tests performed on 'as is' and pulverized 'high' and 'low' grade tails gave the same recovery in each case (~ 50%). This indicates that in both tailings samples there is gold amenable to cyanidation as well as submicroscopic gold in the sulphides.

The gold recovery by direct cyanidation with **no regrind** from the 1st and 2nd Maxwell cell concentrates was **23%** and **32%** respectively. After regrinding to 100 - 200 mesh the recoveries increased to **35%** and **36%** respectively. The cyanidation results indicate that most of the gold in both concentrates is refractory and that grinding has little effect upon recovery. The gold

recovered by direct cyanidation from the rougher and the scavenger concentrates was respectively 29% and 25%.

Finally, cyanidation of the roaster calcine sample, assaying 92.1 g/t Au, 'as is' and after regrinding gave similar in Au content (4.1 and 3.8 g/t Au) residues. This indicates that the refractoriness of the gold in the roaster calcine is not due to locking.

## 3.3 SULPHIDE MINERALOGY

Pyrite and arsenopyrite are the main sulphides in the GIANT Yellowknife ore (Table 7). Combined they account for 95%+ of the sulphides. Marcasite ($FeS_2$), chalcopyrite ($CuFeS_2$), sphalerite ( (Zn,Fe)S), acanthite ($Ag_2S$), boulangerite ($Pb_5Sb_4S_{11}$), tetrahedrite ($Cu_{12}Sb_4S_{13}$), berthierite ($FeSb_2S_4$), gudmundite (FeSbS) and stibnite ($Sb_2S_3$) are present in trace amounts. In addition native Sb was noted.

There are two types of arsenopyrite, coarse-grained and fine-grained (Plate 1). The fine-grained arsenopyrite is more abundant than the coarse-grained type in the flotation tailings, the light fractions from density separations and in the scavenger concentrate (Table 8).

## 3.4 GOLD MINERALOGY - GOLD MINERALS

In total 487 grains of native Au were observed in the 54 sections studied by optical microscopy (Table 9). Results are given in Appendix A3.

TABLE 7 - NORMATIVE SULPHIDE MINERALOGY (wt%)

| SAMPLE | PYRITE | | ARSENOPYRITE | |
|---|---|---|---|---|
| | 1st estimate | 2nd estimate | 1st estimate | 2nd estimate |
| classifier o/f | 3.14 | 3.15 | 1.93 | 1.89 |
| 'high' grade tails | 0.31 | 0.31 | 0.18 | 0.18 |
| 'low' grade tails | 0.23 | 0.23 | 0.14 | 0.13 |
| 1st Max. cell conc. | 46.2 | 50.7 | 25.9 | 25.2 |
| 2nd Max. cell conc. | 55.1 | 60.2 | 25.0 | 24.2 |
| Rougher concentrate | 21.8 | 21.9 | 20.7 | 20.3 |
| Scavenger concentrate | 6.37 | 6.40 | 6.56 | 6.47 |

The arsenic concentration in the pyrite is 0.68 wt.%

TABLE 9 - SUMMARY ON OPTICAL MICROSCOPY OF GOLD

| SAMPLE | # OF SECTIONS | # OF GRAINS | ESTIMATE VISIBLE Au CONCN. (ppm) |
|---|---|---|---|
| Classifier o/f | | | |
| +200 sink | 8 | 198 | 94.7 |
| +200 int. | 5 | 5 | 2.2 |
| -200 sink | 5 | 15 | 23.4 |
| High grade tails | | | |
| +200 sink | 5 | 5 | 13.1 |
| -200 sink | 1 | 1 | 25.8 |
| Low grade tails | | | |
| +200 sink | 5 | 3 | 0.4 |
| -200 sink | 1 | 0 | - |
| 1st Maxwell conc. | | | |
| +200 | 3 | 41 | 185.0 |
| -200 | 3 | 56 | 78.9 |
| 2nd Maxwell conc. | | | |
| +200 | 3 | 48 | 632.8 |
| -200 | 3 | 44 | 41.7 |
| Rougher conc. | | | |
| +200 | 3 | 25 | 54.2 |
| -200 | 3 | 29 | 62.0 |
| Scavenger conc. | | | |
| +200 | 3 | 6 | 3.5 |
| -200 | 3 | 8 | 1.8 |
| TOTAL | 54 | 487 | |

Four distinct mineralogical associations of native gold were identified: (i) liberated; (ii) with or within pyrite particles; (iii) with or within coarse-grained arsenopyrite; and (iv) enclosed or combined with fine-grained arsenopyrite or arsenopyrite/quartz middling particles. Less common associations noted are combination with pyrrhotite, acanthite and stibnite.

Enclosed gold particles are typically rounded to oblate with the exception of a few grains enclosed in the coarse-grained arsenopyrite which occupy fractures (Plate 2). There is a marked association of native Au with sulphosalts and acanthite with small quantities of those minerals accompanying gold within inclusions or indeed enclosed within larger gold grains.

The composition of the gold grains is that of native Au with an average Ag content of 6.9 ± 1.2 wt% (based on EDX analysis of 112 grains). There is no apparent relationship between the native Au grain size and its Ag content. The Ag concentration range is from 0.0 to 26.2 wt%. The gold grains associated with the coarse-grained arsenopyrite have a higher Ag content than those associated with either pyrite or the fine-grained arsenopyrite. Those grains with > 20% Ag occur exclusively in this association. The largest (liberated) grains have a fairly narrow range of Ag content from 6 - 10 wt% (Figure 7). Both the rate of flotation and of dissolution in cyanide are affected adversely by an increased Ag content.

The native Au characterization in terms of grain size and association was performed on sized density fraction in order to facilitate the optical examination. Results are given in Appendix A3.

### 3.4.1 Characterization of native Au in the classifier o/f (sample #1)

+200 mesh sink fraction

The +200 mesh sink fraction assayed 87.2 g/t Au and represents 2.45% by weight of the classifier o/f sample. Therefore, it accounts for 24.5% of the Au head assay.

Six out of 195 native Au grains identified in the +200 mesh fraction accounted for 75% of the total Au visually estimated and had an average size of 3109 $\mu m^2$ area.

The 50 grains enclosed in pyrite, and the 4 grains combined with pyrite accounted for 10.7% of the visually estimated gold with an average size of 49 $\mu m^2$.

The 28 grains enclosed in coarse-grained arsenopyrite and 18 combined accounted for 5.7% of the total gold area and had an average size of 31 $\mu m^2$.

The 89 grains enclosed in fine-grained arsenopyrite and within aggregate particles of fine-grained arsenopyrite and quartz accounted for 8.6% of the visually estimated gold (Plate 3). The average size of the gold

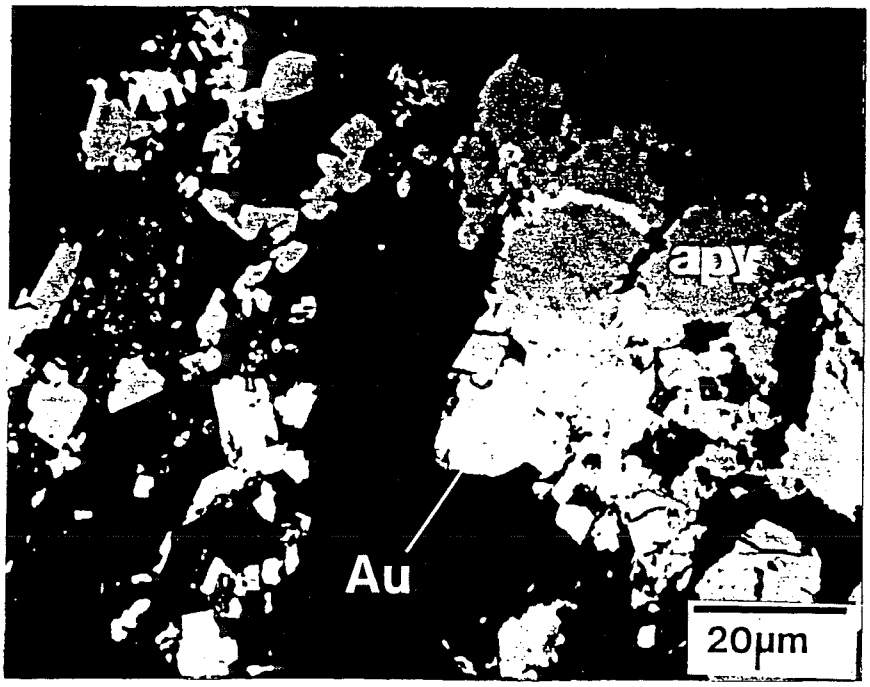


Native Au associated with fine-grained arsenopyrite

PLATE 3

grains was 24 $\mu m^2$. The gold grains are frequently present at the interface between quartz and arsenopyrite (one of the causes for losing cyanidable Au to the flotation tails).

The size distribution of the native Au grains clustered in terms of their association in the +200 mesh sink fraction is depicted in Figure 8. The cumulative frequency diagram in Figure 9 stresses the coarseness of the liberated native Au grains. The unliberated gold grains are much smaller and have very similar size distribution curves. For every association (with pyrite, coarse or fine arsenopyrite) native Au grains finer than 100 $\mu m^2$ make 8% of the gold in that association.

+200 mesh intermediate density fraction (2.7 - 3.0 g. $cm^{-3}$)

In this size fraction report quartz/sulphide middling particles with the sulphide making 2 to 15 wt.% of the particle. These particles typically will report to the tailings. Studying this fraction revealed the importance of the native Au associated with middling particles. All 8 native gold grains were enclosed in the fine-grained arsenopyrite-quartz particles and were less than 80 $\mu m^2$ in size.

Cyclosizer cones 1 - 3 (73. - 20.$\mu$m)

The sink fraction did not contain as much gold as the +200 mesh sink fraction (either in terms of number of gold grains or total visually estimated gold). In total 15 native gold grains were identified. The 6 liberated grains accounted for 75.3% of the visually estimated gold in this fraction.

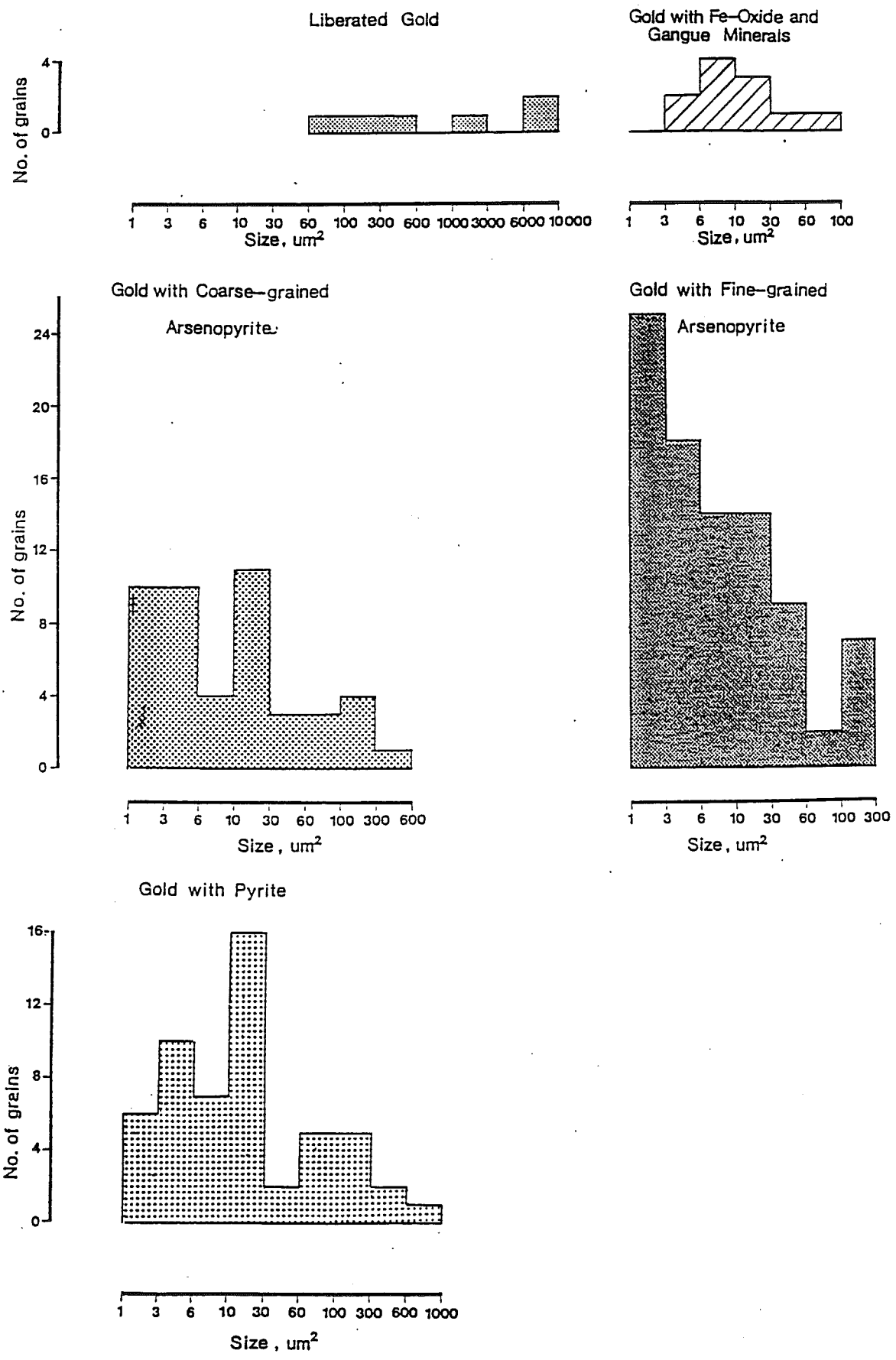


FIGURE 8 - Association and size distribution of native Au

Cyclosizer cones 4 + 5 + discharge (< 20. $\mu$m)

The finest unseparated by density size fraction assayed 3.4 g/t Au which is only 38% of the head assay. Optical microscopy of the two coarser size fractions has shown that the number of gold grains and the total visually estimated gold decreases in the finer size fractions. **Most of the assayed Au in the finest size fraction is submicroscopic within arsenopyrite.**

### 3.4.2 Characterization of native Au in the 'high' grade and 'low' grade flotation tailings (sink fraction)

The 'high' grade tailings assay 0.65 g/t Au and the 'low' grade 0.48 g/t Au. The sink fractions of the +200 mesh and 1 - 3 cones of the cyclosizer (73. - 21. $\mu$m) were used to preconcentrate the sulphides and the visible Au associated with them. The specific gravity of the heavy liquid was 2.8 g. $cm^{-3}$. At this specific gravity middling particles with 5 wt.% sulphide sunk.

**In the 'high' grade tails, 6 native Au grains were identified.** Three grains were combined with quartz, one enclosed in quartz and the remaining 2 were enclosed in fine-grained arsenopyrite/quartz middling particles. The average size of 3 native Au grains combined with quartz was 526 $\mu m^2$ with the remaining grains being smaller than 30 $\mu m^2$. **The coarser native Au grains that are combined with quartz is the main difference observed between the 'high' and 'low' grade tails.** These grains are recoverable by direct cyanidation without regrind.

Three native Au grains were identified in the 'low' grade tails. The average grain size was 12 $\mu m^2$ and all were enclosed in fine-grained arsenopyrite/quartz middling particles.

### 3.4.3 Characterization of native Au in the four concentrate samples

Six sections from each concentrate sample were examined to characterize the native Au (Table 9). The number of native Au grains identified were as follows: 97 in the concentrate from the 1st Maxwell cell, 92 grains in the 2nd Maxwell cell concentrates, 54 grains in the rougher concentrate and 14 in the scavenger concentrate.

The size distribution and mineralogical association of native gold in the concentrates is consistent with that in the classifier o/f. A shifting trend in the mineralogical association of the gold grains is noted from the concentrate from the 1st Maxwell cell to the scavenger concentrate (Figure 10).

The liberated gold grains are recovered in the 1st and 2nd Maxwell cells and the rougher concentrate, but were not observed in the scavenger concentrate. Liberated gold grains account for the highest percentage of the visually estimated gold in the 2nd Maxwell cell concentrate. In the 1st Maxwell cell and the rougher concentrates liberated gold accounts for more than 75% of the observed native Au. Very large (>10,000$\mu m^2$) gold grains float in the Maxwell cells as well as smaller grains (Appendix A3).

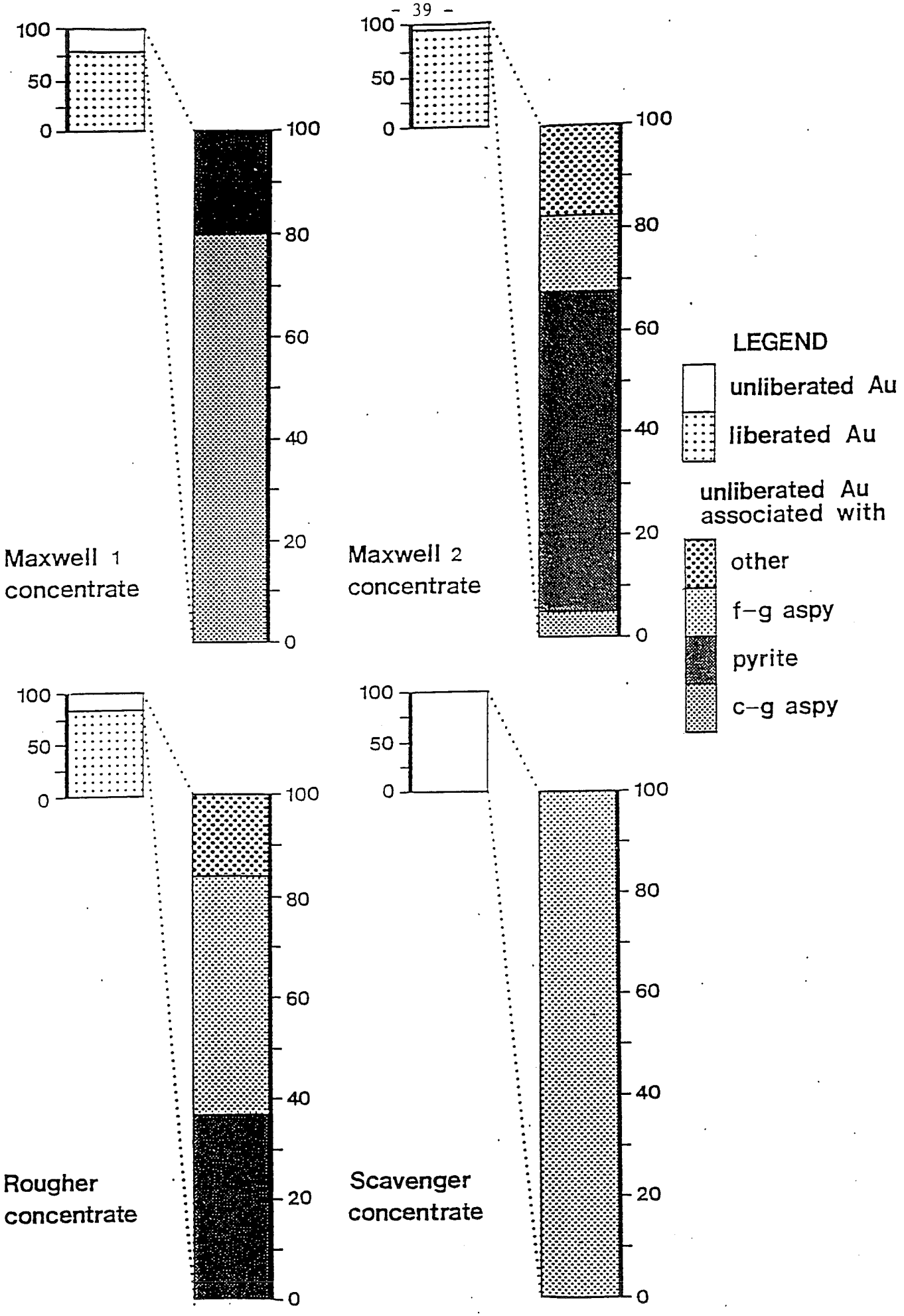


FIGURE 10 - Distribution of native Au based on association in the GIANT concentrates

The unliberated native Au grains represent the following fractions of the visually estimated Au in the four concentrates: 20% 1st Maxwell, 5% 2nd Maxwell, 20% in the rougher and 100% in the scavenger concentrate.

Native Au associated with coarse-grained arsenopyrite is recovered in the 1st Maxwell cell, and represents 80% of the unliberated gold in this concentrate. In the 2nd Maxwell cell it represents only 15% (Figure 10).

Native Au associated with pyrite has been observed in the two Maxwell cell concentrates and the rougher concentrate but not in the scavenger concentrate. It accounts for more than 60% of the unliberated gold in the 2nd Maxwell cell, 35% in the rougher concentrate and 20% in the 1st Maxwell cell concentrate (Figure 10).

Interestingly, the native Au associated with the fine-grained arsenopyrite (Figure 10) is not recovered at all in the 1st Maxwell cell and is only present in minor quantities (15% of the unliberated Au) in the 2nd Maxwell concentrate. The proportion of visible Au in this association increases from 45% of the unliberated gold in the rougher concentrate to 100% of the native gold in the scavenger concentrate. It is emphasized that all native gold (14 grains) in the scavenger concentrate were associated with fine-grained arsenopyrite. Obviously the recovery of the unliberated native Au reflects the flotation behaviour of the host sulphide. It is worth remembering that native Au lost to the tailings is associated with quartz or with fine-grained arsenopyrite.

In the concentrate samples, there is a marked decrease in apparent concentration of native Au with fineness of sample. This is consistent with observations in the classifier o/f and the expected distribution of a mineral with a high specific gravity (gold) in a cyclosized sample.

## 3.5 CALCINE MINERALOGY

Maghemite ($\alpha$-$Fe_2O_3$), magnetite ($Fe_3O_4$), hematite ($\gamma$-$Fe_2O_3$) and goethite (FeO.OH) are the main oxide phases. Ferric arsenate (scorodite) is the principal arsenic mineral. Pyrite, pyrrhotite and in smaller amounts arsenopyrite are present in the cores of the relatively uncommon partially oxidized particles. The pyrrhotite is an intermediate oxidation product of the arsenopyrite and pyrite oxidation.

The sequence of intermediate stages of oxidation of a sulphide particle (pyrite or arsenopyrite) shown in Figure 11 was compiled from observations made on the GIANT Yellowknife roaster calcine. At first pores develop on the outer zone of the pyrite particle, then a layer of fine-grained pyrrhotite forms, which soon is oxidized giving formation to a layer of magnetite and then maghemite. The final oxidation product is hematite. Most of the magnetite/maghemite layers display relatively large concentric pores with lesser radiating micropores. Arsenopyrites tend to form the pyrrhotite layer first which frequently reaches considerable thickness before converting to iron oxide. Part of the arsenic is fixed as ferric arsenate closely intergrown with the pyrrhotite.

1. Unoxidized pyrite particle

2. Incipient oxidation: formation of thin magnetite layer

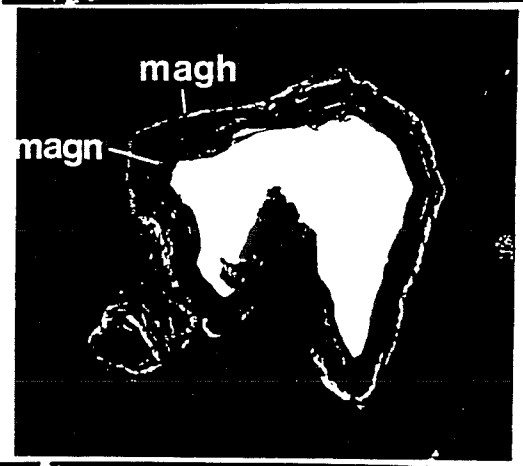


3. Intermediate oxidation: double oxidation layer (pyrite/ magnetite/maghemite)

4. Advanced oxidation: isolated sulphide in the centre of the calcine particle.

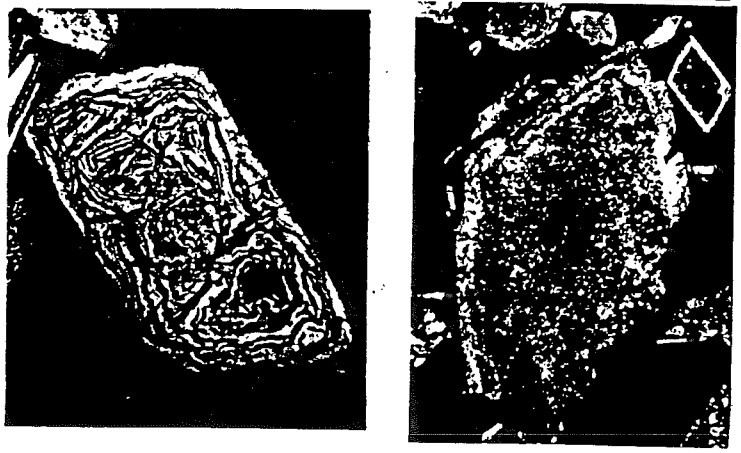

5.6. Complete oxidation: impermeable maghemite (5) and permeable goethite/scorodite particle (6) with partially sintered rim.

FIGURE 11 - Schematic of sequence of arsenopyrite (pyrite) oxidation in the GIANT Yellowknife roaster

The mineralogical examination of the roaster calcine was beyond the scope of this study. The brief examination was made to provide the required basis for studying the gold distribution in the calcine and calcine residue.

## 3.6 GOLD MINERALOGY: SUBMICROSCOPIC OR 'INVISIBLE' Au

The term 'invisible' Au is synonymous to submicroscopic Au and denotes gold that is too fine for characterization by scanning electron microscopy (less than 0.1 $\mu$m (1000Å) in diameter). The 'invisible' Au can be of **colloidal size**, 10 to 1000Å in diameter **particulate Au** or **solid solution** Au. Colloidal Au is detectable by high resolution Transmission Electron Microscopy (TEM) or if coarser than 500Å by ion probe microanalysis. Colloidal Au occurs typically in oxidation products of Au-bearing sulphides. Solid solution Au occurs in the crystal structure of arsenian pyrite and arsenopyrite. Since it is chemically combined, it requires the complete destruction of the sulphide crystal structure in order to be recovered.

### 3.6.1 Mill and flotation plant samples

In addition to pyrite and arsenopyrite the main sulphide minerals in the GIANT Yellowknife ore, marcasite, pyrrhotite, tetrahedrite, chalcopyrite and berthierite were analyzed for 'invisible' Au.

In the GIANT Yellowknife ore the **submicroscopic Au concentrates preferentially in the arsenopyrite**. In 8 out of 105 arsenopyrite grains gold concentrations higher than 1000 ppm (g/t) were recorded (Table 10). The average submicroscopic Au content of 105 arsenopyrites is 229 ppm

TABLE 10 - SUBMICROSCOPIC Au (ppm) IN ARSENOPYRITE - GIANT YELLOWKNIFE

| Particle # | Au,ppm | Particle # | Au,ppm | Particle # | Au,ppm |
|---|---|---|---|---|---|
| 2s | 25. | 79s | 4.0 | 149 | 4.1 |
| 4s | 640. | 80 | 0.99 | 156 | 31. |
| 7s | 490. | 81s | 1,600. | 157b | 1.6 |
| 11s | 210. | 82b | 2.3 | 159s | 1,000. |
| 14 | 220. | 83b | 62. | 162 | 25. |
| 16s | 490. | 86 | 38. | 164 | 7.0 |
| 18 | 320. | 90 | 54. | 173s | 100. |
| 19 | 10. | 93b | 1,200. | 174s | 56. |
| 20 | 3.1 | 95 | 96. | 176c | 38. |
| 22 | 2.9 | 96 | 1.4 | 177f | 1,100. |
| 23s | 30. | 103s | 1,400. | 179s | 490. |
| 26 | 54. | 104s | 250. | 183 | 100. |
| 29b | 18. | 107s | 1,300. | 185s | 230. |
| 33b | 8.2 | 110s | 480. | 186 | 0.56 |
| 34b | 7. | 118 | 29. | 190s | 2,100. |
| 35b | 11. | 119s | 19. | 191 | 160. |
| 37s | 11. | 120s | 10. | 192 | 4.5 |
| 38s | 50. | 121s | 270. | 195 | 10. |
| 39 | 21. | 123 | 59. | 200 | 50. |
| 41 | 47. | 127 | 230. | 201 | 110. |
| 42 | 1,200. | 133 | 14. | 202 | 5. |
| 47b | 1.2 | 134 | 18. | 203 | 25. |
| 48b | 1.8 | 135 | 2.1 | 205 | 43. |
| 49 | 17. | 136 | 78. | 209s | 680. |
| 50b | 90. | 137 | 2.6 | 211s | 410. |
| 57s | 250. | 138 | 1.2 | 212b | 7.0 |
| 59s | 230. | 140 | 270. | 218s | 1,300. |
| 72 | 18. | 144 | 11.5 | 219 | 130. |
| 76 | 350. | 145 | 600. | 222 | 70. |
| 77 | 25. | 146s | 350. | 223m | 160. |
| 78 | 50. | 147s | 410. | 224s | 520. |
| 230 | 2,500. | 148 | 640. | 229s | 2,900. |
| 232s | 37. | | | 236 | 5.8 |
| 233vf | 600. | | | 238 | 7.8 |
| 234vf | 480. | | | 244b | 330. |
| 235 | 16. | | | 245s | 450. |
| | | | | 249 | 700. |

| | n | $\hat{x}$ | $\lambda$ | MIN | MAX |
|---|---|---|---|---|---|
| | 105 | 299.03 | 101.33 | 0.56 | 2,900 |
| fine | 37 | 494.6 | 164.2 | 4.0 | 2,900 |
| coarse | 68 | 153.3 | 90.4 | 0.56 | 1,200 |

s: fine-grained, b: blastic, vf: very fine grained

with a confidence interval of 101 ppm at the 95% significance level. The fine-grained arsenopyrite (Plate 1) has a higher average submicroscopic Au content 495 ± 164 ppm compared to the coarse-grained arsenopyrite 153 ± 90 ppm (Figure 12). The range of Au concentrations in the coarse arsenopyrite is broader than that of the fine-grained arsenopyrites because there are only coarse-grained arsenopyrites with low gold contents (Figure 12).

The GIANT Yellowknife pyrite, has a low arsenic content. The average arsenic content of 99 pyrite grains was 0.68 ± 0.16 wt%. Therefore its potential submicroscopic gold content is as expected low (Figure 14). The average submicroscopic gold concentration in 96 pyrites is 4.7±1.24 ppm. The pyrite grains with arsenic content higher than 1 wt% were gold-bearing (Table 11). Fifteen arsenic/gold-rich pyrites were analyzed. The maximum gold content recorded in the Yellowknife pyrite was 42 ppm, and the minimum was below the minimum detection limit, that is less than 0.28 ppm Au (Figure 13).

Marcasite is more enriched in submicroscopic gold compared to pyrite. Two marcasite grains had gold contents of 190 ppm and 1000 ppm. Excluding these grains the average gold content of the GIANT Yellowknife marcasite is 5.9 ± 3.0 ppm.

Tetrahedrite and berthierite combined are the second in importance trace minerals in the GIANT Yellowknife ore. With the exception of two particles containing submicroscopic Au in significant amounts 90 ppm and 330 ppm the average gold content of the rest is 1.2 ± 0.6 ppm.

TABLE 11 - SUBMICROSCOPIC Au (ppm) AND As (wt%) IN PYRITE - GIANT YELLOWKNIFE

| Particle # | Au, ppm | As, wt% | Particle # | Au, ppm | As, wt% |
|---|---|---|---|---|---|
| 1 | 0.1 | 0.15 | 66 | 0.13 | 0.21 |
| 3 | 0 | 0.13 | 67 | 2.0 | 0.58 |
| 5 | 0.47 | 0.12 | 69 | 0.12 | 0.98 |
| 9 | 0.12 | 0.21 | 70 | 0.35 | 0.12 |
| 12 | 13.0 | 2.5 | 73 | 1.8 | 0.15 |
| 13 | 0.1 | 2.0 | 75 | 0.23 | 0.12 |
| 15 | 0.29 | 0.32 | 84b | 1.7 | 0.27 |
| 17 | 0.43 | 0.28 | 85 | 7.7 | - |
| 21 | 0.27 | 0.18 | 87 | 0.16 | 0.19 |
| 24 | 0.21 | 0.11 | 88 | 1.7 | 0.25 |
| 28b | 1.0 | 0.16 | 91 | 0.43 | 0.15 |
| 40 | 0.8 | 0.62 | 94 | 14.0 | 2.3 |
| 43 | 1.0 | 3.0 | 97 | 0.67 | 0.08 |
| 44 | 0.8 | 0.72 | 98 | 2.8 | 0.66 |
| 46 | 0.17 | 0.042 | 99 | 0.57 | 1.3 |
| 51 | 0.16 | 0.12 | 100 | 3.4 | 0.54 |
| 52b | 11.0 | 0.18 | 101 | 0.37 | 0.29 |
| 53 | 27.0 | 0.2 | 102b | 4.6 | 0.09 |
| 54 | 0.12 | 0.22 | 105 | 0.37 | 1.3 |
| 55b | 1.3 | 0.47 | 111 | 4.0 | 2.7 |
| 56b | 1.2 | 0.38 | 112 | 1.5 | 0.28 |
| 58 | 0.23 | 0.2 | 113 | 0.27 | 0.32 |
| 60 | 5.9 | 1.6 | 114 | 0.67 | 0.15 |
| 61b | 4.9 | 0.98 | 115 | 0.87 | 0.12 |
| 62 | 0.8 | 0.26 | 116 | 0.57 | 0.2 |
| 63 | 0 | 0.24 | 117 | 9.1 | 2.2 |
| 65 | 13.0 | 2.6 | 122 | 5.9 | 0.98 |
| 124 | 1.6 | 0.21 | 182b | 5.7 | 0.45 |
| 125 | 0.67 | 0.09 | 184 | 2.2 | < 0.01 |
| 128 | 0.33 | 0.17 | 187 | 2.7 | 0.19 |
| 129 | 9.1 | 0.14 | 188 | 1.8 | 0.22 |
| 142 | 2.3 | 1.2 | 193 | 3.0 | 2.8 |
| *139 | 1700. | 2.6 | 194 | 41.0 | 1.2 |
| 141b | 5.7 | 0.066 | 196s | 18.0 | - |
| 143 | 0.67 | 0.25 | 197 | 15.0 | 2.2 |
| 150 | 1.4 | 0.21 | 198 | 1.8 | 0.29 |
| 151 | 1.8 | 1.8 | 199 | 1.8 | 0.12 |
| 152 | 1.0 | 0.1 | 206 | 1.2 | 0.31 |
| 153 | 1.3 | 0.032 | 207 | 19.0 | 2.5 |
| 154 | 2.0 | 0.89 | 208 | 2.4 | 0.84 |
| 155 | 8.9 | 1.8 | 215 | 1.8 | 0.14 |
| 158 | 34.0 | - | 216s | 14.0 | 0.98 |
| 161 | 1.4 | 0.09 | 217 | 8.9 | 0.46 |
| 166 | 1.6 | 0.6 | 221 | 1.3 | - |
| 167 | 2.6 | 0.12 | 225 | 4.1 | 1.7 |
| 168 | 22.0 | 0.98 | 228s | 3.2 | 1.7 |
| 169 | 2.1 | 0.09 | 231 | 12.0 | 0.0089 |
| 170 | 1.4 | < 0.009 | 237 | 8.7 | 1.7 |
| 171 | 1.7 | 1.1 | 250 | 0.8 | 0.09 |
| 172 | 2.4 | 0.13 | 256 | 33.0 | 0.28 |
| 178 | 8.7 | 1.8 | 257 | 1.8 | 0.021 |

| | n | $\hat{x}$ | ± | λ | MAX | MIN |
|---|---|---|---|---|---|---|
| *without Au | 101 | 4.7 | ± | 1.5 | 41.0 | - |
| As | 99 | 0.68 | ± | 0.16 | 3.0 | - |

The submicroscopic gold concentration in the pyrrhotite and chalcopyrite is insignificant, 1.1 ± 0.5 ppm and 0.8 ± 0.5 ppm respectively. The ion probe data on the submicroscopic gold concentration in the minor sulphides are given in Table 12.

### 3.6.2 Roaster Calcine (#14)

The roaster calcine assayed 91.7 ± 0.4 g/t Au. Examination of the sample by optical microscopy did not reveal native Au in any appreciable amount. However, ion probe microanalysis detected submicroscopic gold in the calcine particles. Subsequent examination by SEM of the most enriched in gold particles resulted in the identification of colloidal Au in some (Plate 4).

In total 30 roaster calcine particles were analyzed for gold with the ion microprobe. Results are given in Table 13. Arsenic was also monitored but a calibration curve is not yet available for arsenic. The maximum gold concentration, 330 ppm, was determined in a maghemite particle showing limited porosity. The minimum gold concentration was 0.55 ppm.

The calcine particles were classified into two groups based on their texture (Figure 14) the relatively impermeable and the relatively permeable particles. The first group is composed predominantly of maghemite particles with a limited number of relatively coarse concentric pores that provide little overall permeability (Plate 5). The second

TABLE 12 - SUBMICROSCOPIC Au IN MINOR SULPHIDE MINERALS - GIANT YELLOWKNIFE

TETRAHEDRITE & BERTHIERITE

| Grain # | Au, ppm |
|---|---|
| GY 10 | 0.8 |
| 25 | 0.28 |
| 31 | 90. |
| 32 | 0.64 |
| 45 | 1.5 |
| 89 | 0.46 |
| 126 | 330. |
| 130 | 0.98 |
| 131 | 1.4 |
| 181 | 0.6 |
| 189 | 0.9 |
| 204 | 2.6 |
| 213 | 5.2 |
| 239 | 1.0 |
| 240 | 0.9 |
| 241 | 0.68 |
| 242 | 2.1 |
| 243 | 0.68 |
| 247 | 0.25 |

MARCASITE

| Grain # | As,wt% | Au,ppm |
|---|---|---|
| GY 27 | 1.8 | 1000. |
| 30 | 0.56 | 7.8 |
| 36 | 3.3 | 0.76 |
| 68 | 0.98 | 190. |
| 132 | 0.07 | 13. |
| 210 | 0.014 | 3.0 |
| 214 | 0.58 | 5.4 |
| 220 | 0.44 | 2.8 |
| 226 | 0.33 | 4.4 |
| 227 | 0.82 | 15.0 |
| 246 | 0.11 | 3.5 |
| 248 | 0.031 | 2.7 |

PYRRHOTITE

| Grain # | Au, ppm |
|---|---|
| GY 109 | 0.36 |
| 160 | 1.8 |
| 163 | 1.4 |
| 165 | 0.97 |
| 175 | 0.96 |

CHALCOPYRITE

| Grain # | Au, ppm |
|---|---|
| GY 6 | 1.0 |
| 8 | 1.0 |
| 108 | 0.31 |

## TABLE 13 - SUBMICROSCOPIC AU IN CALCINE PARTICLES

### A. ROASTER CALCINE (#14)

| RELATIVELY IMPERMEABLE Particle # | Au, ppm | |
|---|---|---|
| 2 | 1.2 | |
| 3r | 1.3 | |
| 4r | 1.3 | |
| 5r | 13. | |
| 6r | 4.3 | |
| 7r | 2.4 | |
| 8 | 0.95 | |
| 11 | 4.7 | [coll.] |
| 13 | 1.2 | |
| 14 | 330. | [coll.] |
| 16 | 48. | [coll.] |
| 17 | 1.2 | |
| 23r | 190. | [coll.] |
| 25 | 30. | |

| n | $\hat{x}\pm\lambda$ |
|---|---|
| 9 (5 outliers) | 2.1±1.0 ppm |

| RELATIVELY PERMEABLE Particle # | Au, ppm | |
|---|---|---|
| 1r | 16. | |
| 9 | 2.6 | |
| 10 | 1.9 | |
| 12r | 70. | [coll.] |
| 15r | 2.9 | |
| 18r | 9.9 | |
| 19r | 18. | [coll.] |
| 20r | 66. | [coll.] |
| 21r | 2.9 | |
| 22r | 5.5 | |
| 24r | 11. | |
| 26r | 39. | |
| 27r | 0.55 | |
| 28r | 0.67 | |
| 29 | 11. | |
| 30 | 6.9 | |

| n | $\hat{x}\pm\lambda$ |
|---|---|
| 13 (3 outliers) | 6.9±3.2 ppm |

NOTES

r: with sintered impermeable rim
[coll.]: colloidal gold
(or/apy): originally arsenopyrite
outlier: particle with gold concentration greater than average $+3.09\sigma$

| | | |
|---|---|---|
| Mineralogy: | Maghemite; less magnetite, hematite | Goethite, scorodite; less maghemite, hematite |
| Porosity: | Few, large pores concentrically distributed | Many small pores, multi-directional |
| Permeability: (inferred) | LOW | Variable depending on the presence of sintered rim |
| Type: | RELATIVELY IMPERMEABLE | RELATIVELY PERMEABLE |

FIGURE 14 - Classification of calcine particles

group is made of mineralogically more complex particles with goethite, hematite, scorodite, and inclusions of maghemite. These particles have many micropores providing greater and more pervasive permeability (Plate 6).

The average submicroscopic gold concentration of the relatively impermeable particles (mostly maghemite) is 2.1 ± 1.0 ppm. Five out of 14 particles were outliers, indicating that their gold concentration was higher than 2.1 + 3.09 x 1.45 = 6.6 ppm (Table 13). The two particles with the highest gold contents, 330 ppm and 190 ppm had colloidal gold.

The average submicroscopic gold content of the relatively permeable particles is 6.9 ± 3.2 ppm. Three out of 16 particles are outliers with the following gold contents: 70, 66 and 39 ppm. In three out of sixteen particles colloidal gold is definitely present (Table 13). The sintered impermeable rim (Plate 7) is expected to decrease the permeability of the particles (unless reground).

### 3.6.3 Calcine Residue (#16) and Cyanided Roaster Calcine (#15)

The calcine residue (#16) assayed 6.36 ± 0.05 g/t Au. The pulverized cyanided roaster calcine assayed significantly lower 4.29 ± 0.52 g/t Au, indicating that regrind improved recovery, as anticipated based on the SEM study. The gold recovery based on these figures is 93.0% in the plant and 95.3% in the laboratory test (#15).

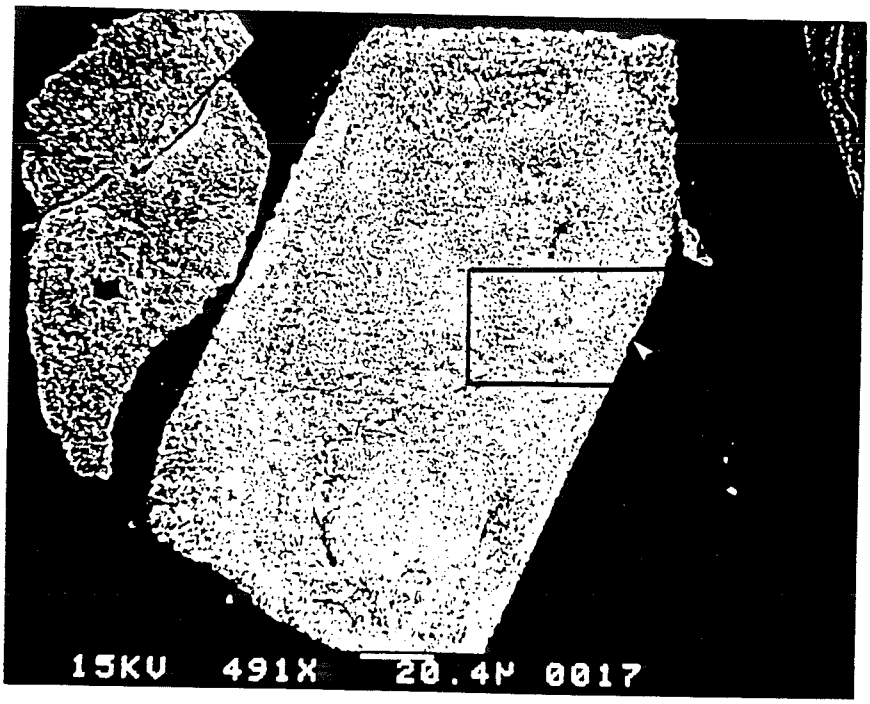


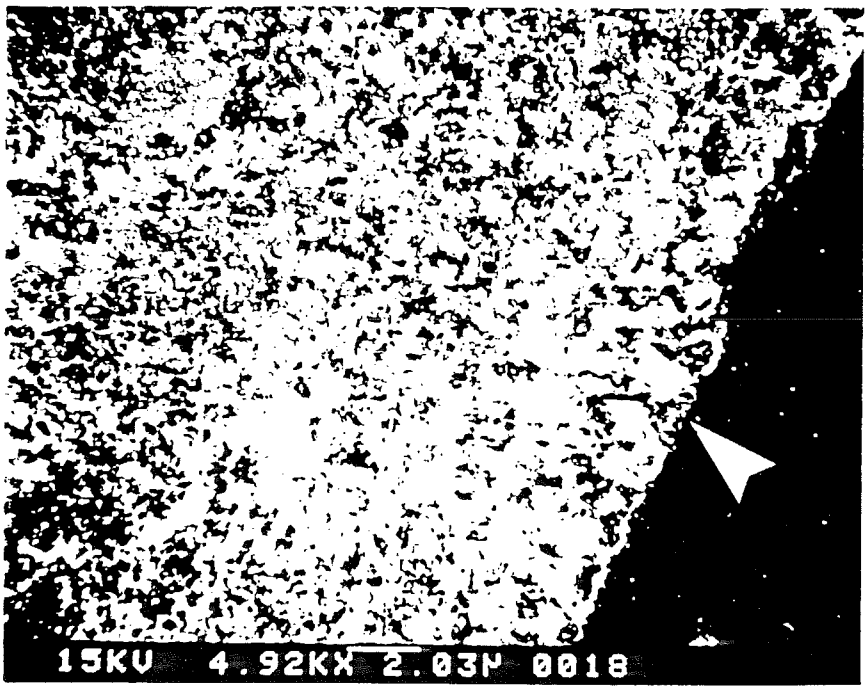


S.E. images of permeable particle.
(Roaster calcine, #14)

PLATE 6

TABLE 13 - SUBMICROSCOPIC AU IN CALCINE PARTICLES

B. CYANIDE LEACHED ROASTER CALCINE (#15)

| RELATIVELY IMPERMEABLE | | | RELATIVELY PERMEABLE | |
|---|---|---|---|---|
| Particle # | Au, ppm | | Particle # | Au, ppm |
| 2 | 1.6 | | 1r | 0.4 |
| 3r | 20. | | 4r | 2.6 |
| 5r | 2.8 | | 7 | 3.1 |
| 6r | 7.9 | | 8 | 13. |
| 11 | 1.6 | | 9r | 4.4 |
| 14 | 0.76 | | 10 | 2.0 |
| 18 | 23. | [coll.] | 12 | 1.6 |
| 19 | 0.76 | | 13 | 1.3 |
| 20r | 5.6 | | 15r | 4.3 |
| 21r | 6.5 | | 16r | 28. |
| 22r | 15. | [coll.] | 17 | 0.71 |
| 23 | 1.0 | | | |
| n | $\hat{x}\pm\lambda$ | | n | $\hat{x}\pm\lambda$ |
| 9 | 3.2±1.8 ppm | | 9 | 2.3±1.0 ppm |
| (3 outliers) | | | (2 outliers) | |

NOTES

r: with sintered impermeable rim
[coll.]: colloidal gold
(or/apy): originally arsenopyrite
outlier: particle with gold concentration greater than average $+3.09\sigma$

TABLE 13 - SUBMICROSCOPIC AU IN CALCINE PARTICLES

C. CALCINE RESIDUE (#16)

| RELATIVELY IMPERMEABLE Particle # | Au, ppm | |
|---|---|---|
| 7 | 1.7 | |
| 8 | 11. | |
| 9 | 3.4 | |
| 17 | 4.9 | |
| 31 | 7.2 | |
| 33r | 25. | (or/apy) |
| n | $\hat{x}\pm\lambda$ | |
| 4 | 4.3±2.3 ppm | |
| (2 outliers) | | |

| RELATIVELY PERMEABLE Particle # | Au, ppm | |
|---|---|---|
| 6r | 22. | |
| 11 | 6.8 | |
| 12 | 31. | |
| 13 | 5.7 | |
| 14 | 14. | |
| 15 | 3.1 | |
| 16 | 4.1 | |
| 19 | 4.1 | |
| 21 | 8.3 | |
| 22 | 7.4 | |
| 23 | 11. | |
| 24 | 239. | |
| 25 | 9.9 | |
| 26 | 0.69 | |
| 27r | 3.7 | |
| 28 | 8.7 | |
| 29r | 6.8 | |
| 30r | 32. | |
| 32r | 19. | |
| 34r | 4.3 | |
| 35 | 6.5 | (or/apy) |
| 36 | 6.1 | (or/apy) |
| 37 | 9.2 | (or/apy) |
| 38r | 11. | (or/apy) |
| 39r | 1.0 | (or/apy) |
| 40 | 1.8 | (or/apy) |
| 41r | 8.3 | (or/apy) |
| 42 | 2.3 | (or/apy) |
| 43r | 5.1 | |
| 44 | 1.4 | |
| n | $\hat{x}\pm\lambda$ | |
| 25 | 6.0±1.4 ppm | |
| (5 outliers) | | |

NOTES

r: with sintered impermeable rim
[coll.]: colloidal gold
(or/apy): originally arsenopyrite

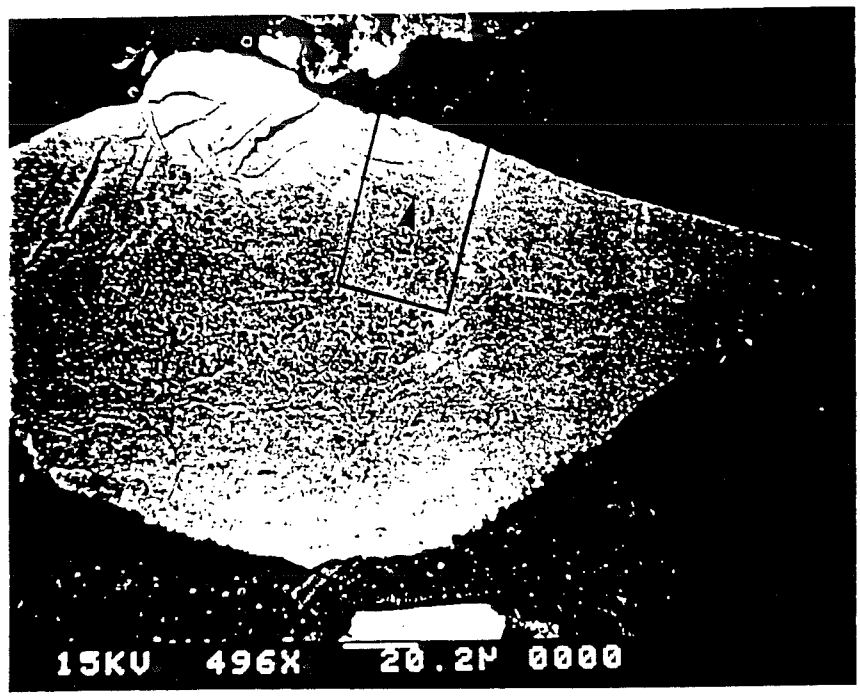


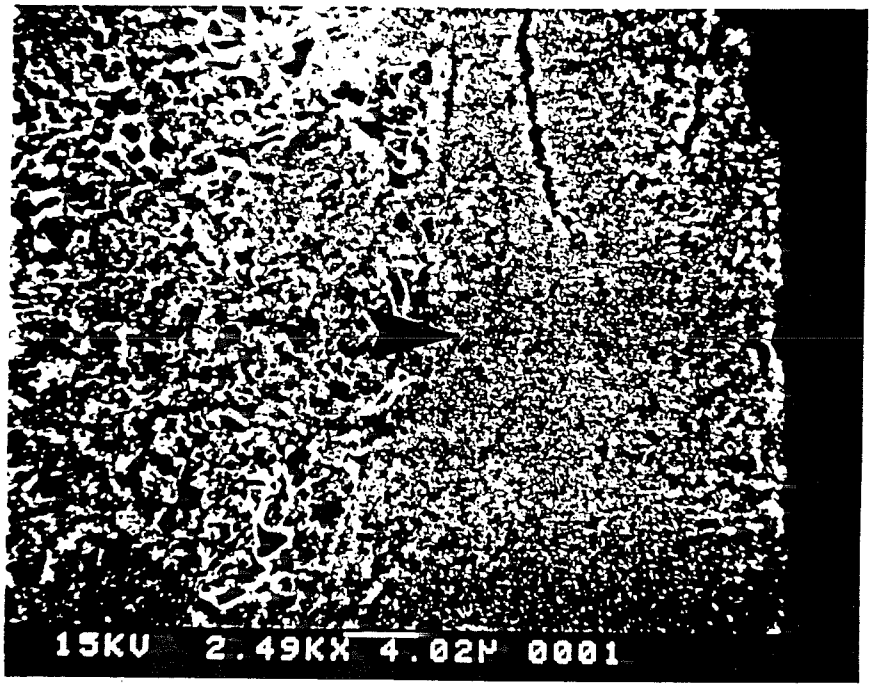


S.E. images of porous calcine particle with impermeable coating

PLATE 7

In total 36 calcine particles from the calcine residue (#16) were analyzed for submicroscopic gold with the ion microprobe (Table 13). The average gold concentration of the **relatively impermeable** particles was 4.3 ± 2.3 ppm with two outliers (11. and 25. ppm Au). This concentration is higher but statistically not different from that in the roaster calcine. The average gold concentration of the **relatively permeable** particles in the **calcine residue is 6.0 ± 1.4 ppm,** marginally lower but statistically the same with that in the roaster calcine. However the gold concentration of the outliers is lower.

Twenty three particles from the cyanide leached roaster calcine were analyzed for submicroscopic gold. The average gold content of the **relatively impermeable** particles is **3.2 ± 1.8 ppm** with 3 out of 12 particles being outliers. The gold content of the outliers (20, 23 and 15 ppm) is comparable to that in the calcine residue indicating that regrind had no effect on these particles. The average gold content of the **relatively permeable** particles is **2.3 ± 1.0 ppm** with 2 out of 11 particles being outliers (13 and 28 ppm). This concentration is lower and statistically different when compared to that of the other samples (#14: 6.9 ± 3.2 ppm, #16: 6.0 ± 1.4 ppm). This indicates that regrinding had a beneficial effect upon the gold recovery.

## 4.0 DISCUSSION

### MINERALOGICAL DISTRIBUTION OF GOLD: CLASSIFIER o/f

Based on direct cyanidation tests it was determined that 41.2% (not normalized) of the gold in the classifier o/f sample, ground to -325 mesh, is directly cyanidable. In the absence of cyanicides and of preg-robbing carbon this figure is considered as the best estimate for the native gold content. Therefore, the refractory to direct cyanidation gold is 58.8% (not normalized). The submicroscopic gold in the arsenopyrite structure was determined independently to be 63.6% of the head assay. This was calculated from the arsenopyrite content of the sample (1.89 wt%) and the average submicroscopic gold concentration in the arsenopyrite (299 ppm) (Appendix A6). The submicroscopic gold in the pyrite is only 1.7% of the head assay. Thus the mineralogically accounted gold comes to 106.5%. The overestimation is attributed primarily to the large confidence interval of the submicroscopic gold concentration in the arsenopyrite.

The gold mineralogical distribution is depicted in the form of a pie diagram in Figure 1a after normalizing the submicroscopic gold to 59.7% The segment representing the gold recovered by direct cyanidation is shown in the second pie diagram with subdivisions based on the native Au associations as determined in the following fractions: +200 sink, +200 intermediate and 1 - 3 cones sink as well as the assays of the float fractions and the slime fraction (3 - 4 cones + discharge). Details are given in Appendices A4 & A5. Thus, the liberated Au accounts for 26.1% of the head assay. The gold associated with arsenopyrite accounts for 4.8%, with pyrite 3.8% and with quartz 4.0% (second pie diagram in Figure 1b).

A further subdivision of the associated native Au was made based on whether the gold is enclosed or combined with the host mineral. This is shown in the third pie diagram in Figure 1c.

Optimum gold recoveries for different combinations of processes may be calculated based on the available data. For example the maximum recovery by sulphide flotation is 100% minus the native Au which is associated with quartz and the part of the submicroscopic Au in the lost arsenopyrite.

MINERALOGICAL DISTRIBUTION OF GOLD: 'HIGH' GRADE TAILINGS

Direct cyanidation of the 'high' grade tails have indicated that 52.2% of the assayed Au (0.72 g/t) is directly cyanidable. Pulverizing the sample had no effect on the gold recovery. Optical microscopy has shown that a significant fraction (69%) of the measured native Au is relatively coarse-grained and combined with quartz (Appendix A3). Therefore it should be recoverable by cyanidation without regrinding. **The refractory to direct cyanidation gold (after pulverizing the sample) is submicroscopic gold in the arsenopyrite.** The amount of gold in the arsenopyrite determined based on the arsenopyrite concentration, the relative abundance of the coarse and fine arsenopyrite in this sample, and their submicroscopic gold concentrations is 74.8%. The normalized gold mineralogical distribution is given in the form of a pie of a grain in Figure 12 and the calculations in Appendix A6.

The gold recovery can be improved by 'pulling' stronger on the fine-grained arsenopyrite in the scavenger concentrate, or by cyanidation of the native Au combined with quartz.

MINERALOGICAL DISTRIBUTION OF GOLD: 'LOW' GRADE TAILINGS

The 'low' grade tailings assay 0.48 g/t Au. Of this 50% is recoverable by direct cyanidation. Pulverizing the sample had no effect on the recovery. The three small (Appendix A3) native Au grains identified were associated with fine-grained arsenopyrite and quartz. As in the 'high' grade tailings the refractory gold is submicroscopic within the arsenopyrite. The submicroscopic gold in the arsenopyrite amounts to 81.3% of the assayed Au. The mineralogically accounted Au is 133.6%. The overestimation is attributed to errors in the arsenic assay and the large confidence interval for the submicroscopic gold within the arsenopyrite. The normalized gold mineralogical distribution in the 'low' grade tailings is given in Figure 12 (second pie diagram) and the calculations in Appendix A6.

Gold losses can be minimized by recovering the gold-rich fine-grained arsenopyrite to the scavenger concentrate. Some of the native Au should also be recovered because of its close association to the fine-grained arsenopyrite (Plate 3). The alternative route would be direct cyanidation without regrind.

## MINERALOGICAL DISTRIBUTION OF GOLD IN THE CONCENTRATES

Samples of the four concentrates, ie. from the 1st and 2nd Maxwell cells, and the rougher and scavenger concentrates were examined to determine the relative importance and flotation behaviour of the two principal gold-carriers: **native Au and the arsenopyrite.**

The mineralogical distributions of gold are depicted in the form of pie diagrams in Figure 3. The results were not normalized. The unaccounted Au in the Maxwell cell concentrates, 3.9% and 10.6%, is attributed to locked fine-grained native Au. Optical microscopy has shown that the enclosed native gold is only a small fraction of the total native gold (Figure 10).

**Arsenopyrite is the principal gold carrier mineral in all four concentrates studied.** Its importance as a gold-carrier increases progressively from the 1st Maxwell cell concentrate to the scavenger concentrate. Thus in the 1st Maxwell cell it accounts for 61.3% of the assayed Au, 56.9% in the second, 68.2% in the rougher and 75.7% in the scavenger concentrate. In the same direction increases the difficulty of recovering the arsenopyrite, because of decreasing grain size. The coarser arsenopyrite floats readily in the Maxwell cell concentrates, while the finer-grained arsenopyrite (which is also more enriched in submicroscopic Au) floats later into the rougher and scavenger concentrates. The significance of the arsenopyrite as a gold carrier is increased further because both arsenopyrite types have locked fine-grained native Au (2.6% of the assayed Au in the classifier o/f). This gold because of its fineness, is not cyanidable and is carried by the arsenopyrite during flotation.

**Native Au is the second most important gold carrier in the GIANT concentrates**, basically accounting for the balance of the assayed Au. **Liberated coarse-grained gold** is recovered in the Maxwell cell concentrates and the rougher concentrate but not the scavenger concentrate. **Gold associated with pyrite** is recovered in the Maxwell and rougher concentrates. **Gold associated with coarse-grained arsenopyrite** is reporting mostly to the 1st Maxwell cell concentrate. On the contrary **native Au associated with fine-grained arsenopyrite** is floating later into the rougher and scavenger concentrates. Therefore, it is obvious that the recovery of the native Au is strongly dependent on its association. The associations in which native Au is lost are the ones which are less floatable, these are native Au associated with quartz and native Au associated with fine-grained arsenopyrite (frequently combined with quartz).

NATURE OF SUBMICROSCOPIC GOLD

As discussed earlier, ion probe microanalysis because of its depth profiling capability is able to differentiate **solid solution** gold from **particulate colloidal gold** down to a certain size. It has been also discussed that the minimum detectable size depend on the sputtering rate, counting time and gold concentration. The distinction between colloidal and solid solution gold is important because the **colloidal gold is cyanidable.** During roasting the solid solution gold in the sulphide structure is expected to redistribute forming colloidal gold in the calcine particles. The distribution and size of the colloidal gold together with the microporosity and permeability of the calcine particle will be important factors controlling the recovery of gold.

However, in addition to the colloidal gold in the calcine produced by oxidation of gold-bearing sulphides, there is also colloidal gold within the sulphide minerals. The 'wavy' pattern of the gold distribution in pyrrhotite, tetrahedrite, berthierite and some pyrite particles from the GIANT ore is a clear indication of colloidal gold. An example is shown in Figure 15. Ignoring the surface layer, there are four gold microinclusions. Based on the operating conditions and $^{197}Au$ count integration the size of each inclusion was determined. The smallest was 400Å in diameter and the largest slightly less than 1000Å. The smallest corresponds to an enrichment of the basal gold concentration (0.62 ± 0.28 ppm) within a layer of 42 $\mu m^3$ by 0.56 ppm; and the largest by 8.4 ppm. The four inclusions increased the total Au content of the grain from 0.62 ppm to 1.03 ppm.

The presence of colloidal gold in the GIANT arsenopyrite is more difficult to prove based on ion probe microanalysis because of the significantly higher gold concentration within arsenopyrite. The 'wavy' pattern of gold distribution in some arsenopyrite grains (Figure 16) is attributed to the inhomogeneous distribution of solid solution gold. This was confirmed by gold ion imaging. In Plate 8 ion images of sulphur, arsenic and gold are shown. The first two are used to mark the grain. The dark hole in the centre of each image is not real. It is attributed to loss of sensitivity in the centre of the imaging system because of the higher fluence in that region. In addition to the inhomogeneous distribution of gold, another important feature to notice is the peripheral distribution of the areas enriched in gold (Plate 8). This observed distribution is with respect

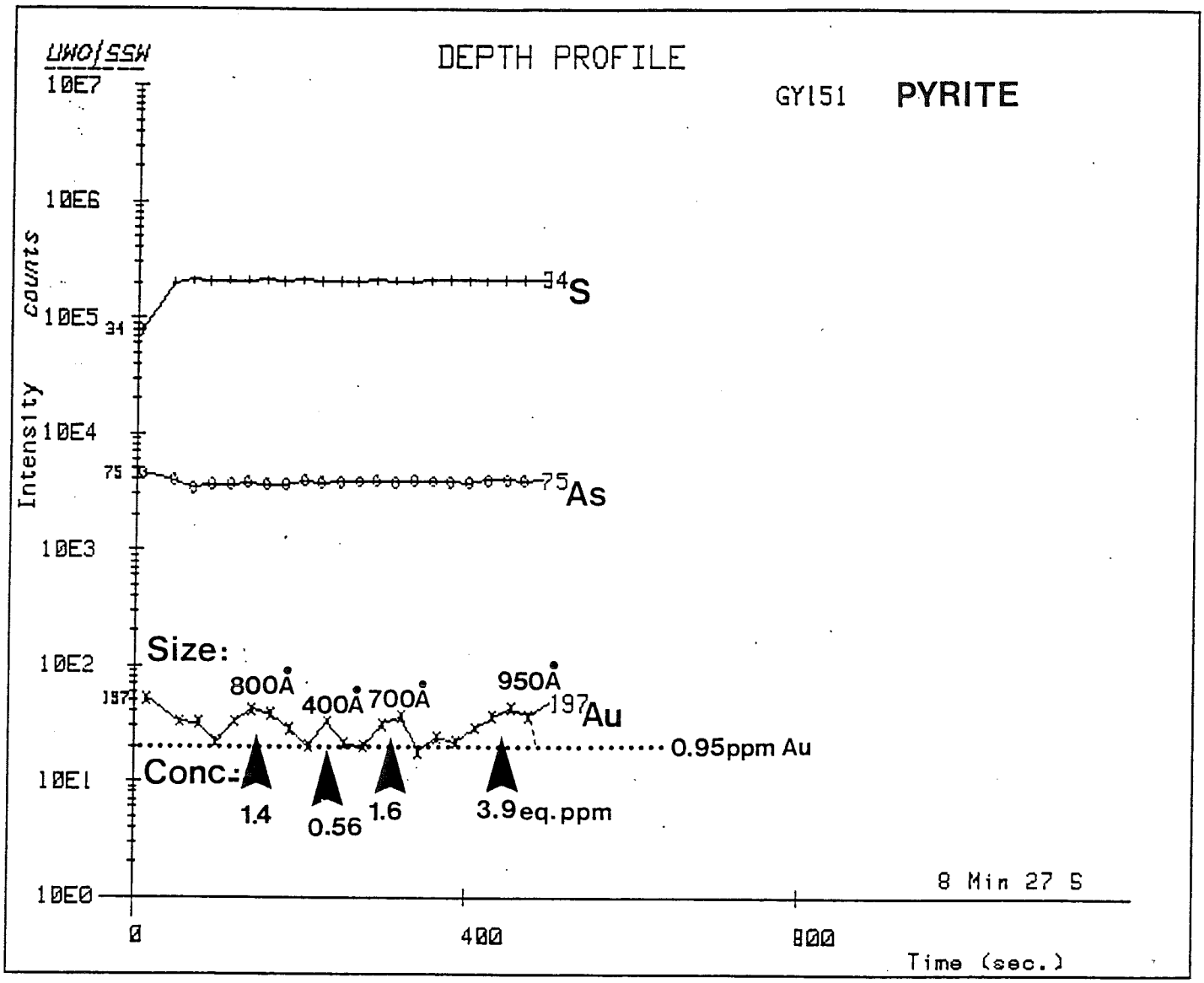


FIGURE 15 - In-depth concentration profile of gold in the Giant pyrite particle #GY 151

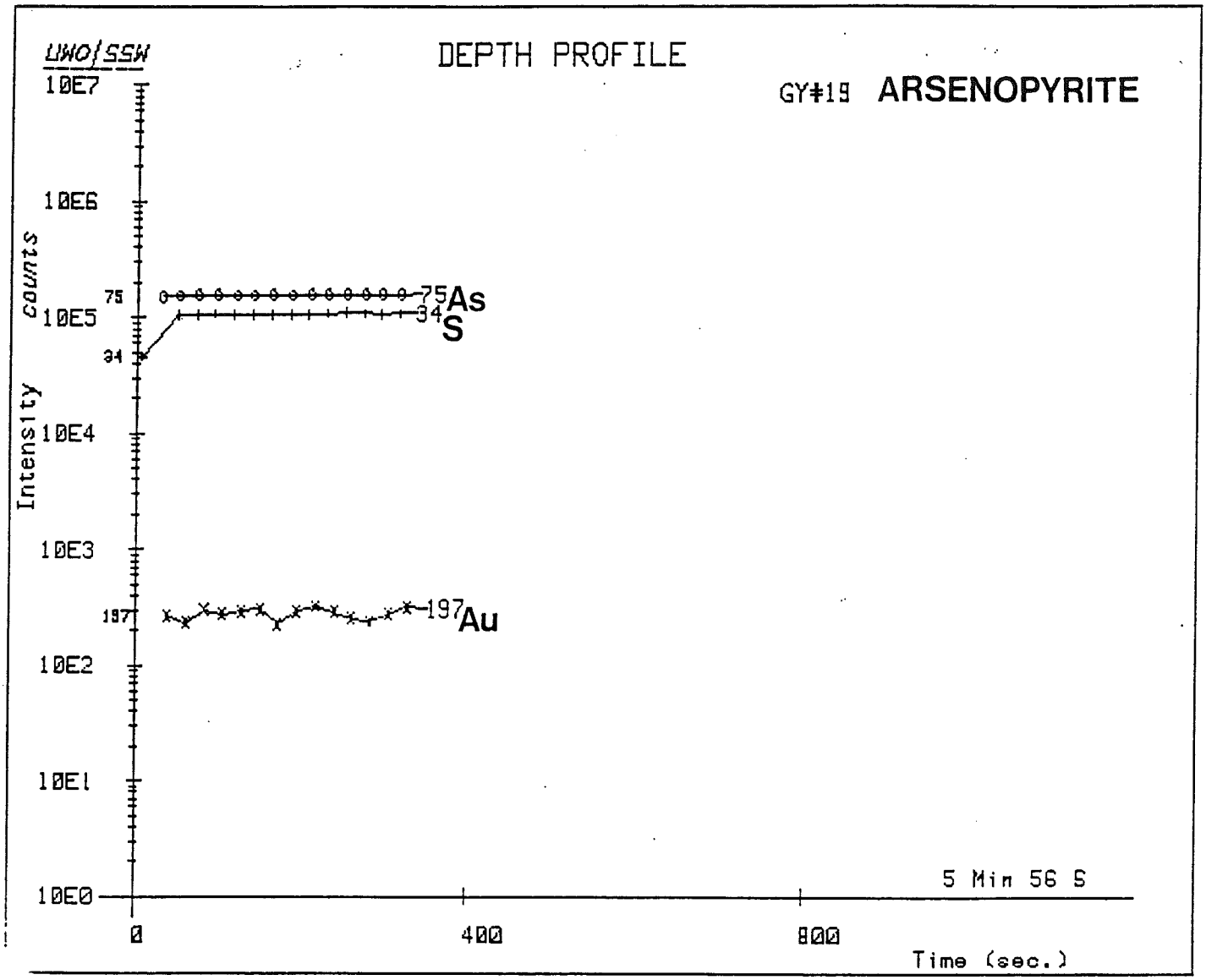


FIGURE 16 - In-depth concentration profile of gold in the GIANT arsenopyrite particle #GY 19

to the original grain boundary, along which separation is likely during grinding. This results in having a significant (not calculated here) fraction of the solid solution gold in the rim of the arsenopyrite particles.

Imaging of gold in calcine particles has shown that the peripheral distribution of gold is inherited in some of the particles (Plates 9 and 10). Such distribution of gold as far as there is no sintering of the rim of the particle is advantageous because the gold can be leached easier and faster. However, if sintering occurs an impermeable layer coats the entire particle, and the gold-rich area may be part of this layer, thus non-recoverable.

## 5.0 CONCLUSIONS

Based on the performed study on the process mineralogy of gold in samples from the flotation circuit (feed, tailings and concentrates), and the roaster and cyanidation plant, the following conclusions can be made:

### A. IMPLICATIONS TO FLOTATION

- Gold is concentrated in two minerals: native Au and arsenopyrite
- The average silver content of the native Au is 6.9 wt.%
- The average submicroscopic gold concentration in arsenopyrite is 299 ppm.
- Native Au contributes 38.7% of the assayed Au, arsenopyrite 59.7% and pyrite only 1.6%.
- Most of the native Au is liberated coarse-grained 67.7%, and floats into the Maxwell cell concentrates and the rougher concentrate
- Of the associated native Au two forms are lost to the tailings: relatively coarse grained combined with quartz (leading to 'high' grade tailings), and combined with fine-grained arsenopyrite ('low' grade tailings)
- The fine-grained arsenopyrite is more enriched in submicroscopic gold (495 ppm) compared to the coarser grained arsenopyrite (153 ppm).

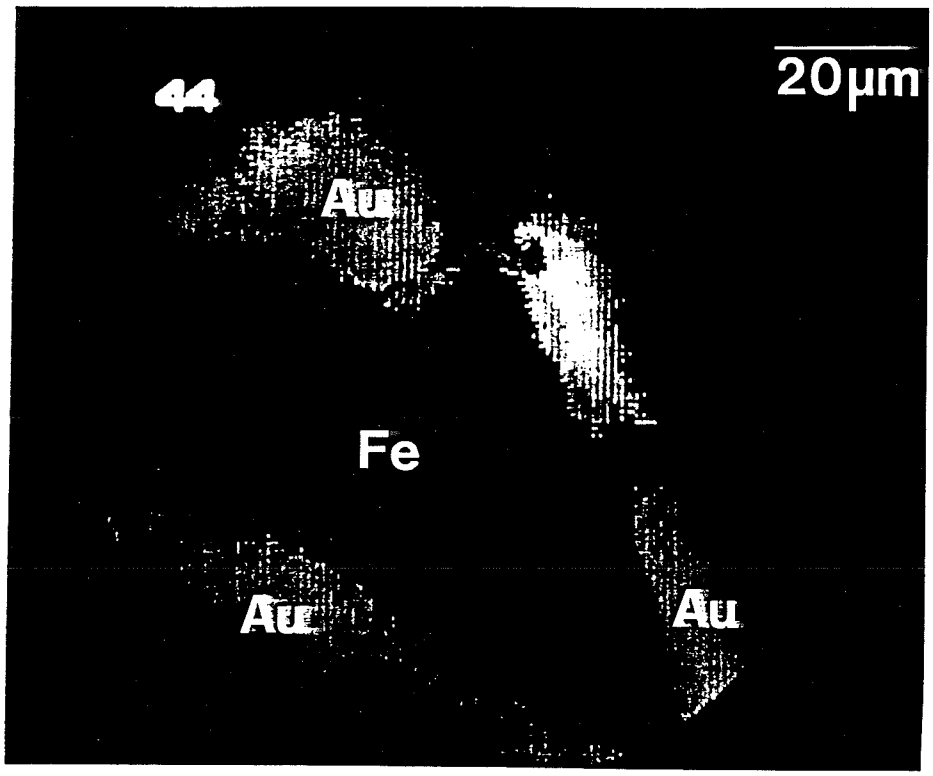


Ion image of iron and gold distribution in calcine particle (#44) from the roaster calcine (#15). The 'invisible' gold is located in the outer zone of the particle.

PLATE 9

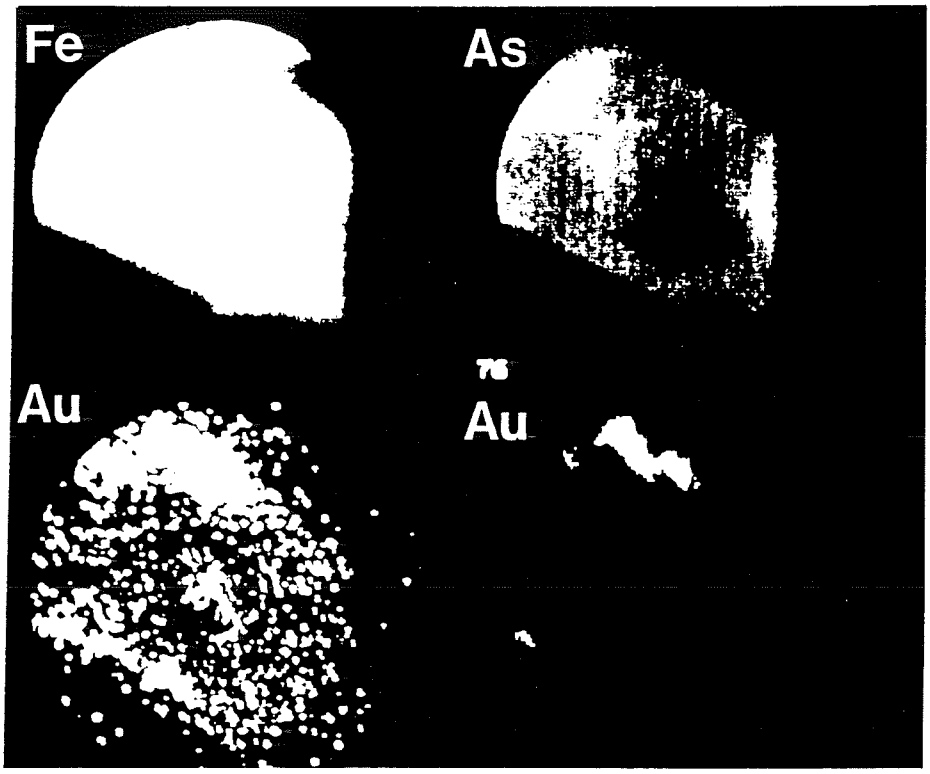


Ion images of iron, arsenic and gold distribution in calcine particle (#18) from the cyanided roaster calcine (#15). The unleached gold is located in the outer zone of the particle.

PLATE 10

- The fine-grained arsenopyrite floats slower, and accounts for 75.5% of the gold in the scavenger concentrate
- **The fine-grained arsenopyrite lost to the tailings results in loss of two forms of gold: submicroscopic gold and fine-grained native gold associated with the arsenopyrite**
- The gold recovery in the flotation circuit can be improved in two ways: (1) by recovering the coarser grained gold associated with quartz, using cyanidation at the present grind or by regrinding the feed to the scavenger concentrate, (2) by recovering more of the fine-grained arsenopyrite (regrind of the scavenger feed).
- Cyanidation of the feed to flotation may improve gold recovery but may also depress some sulphides. If it depresses the fine-grained arsenopyrite gold losses may be considerable. If only pyrite is depressed approximately 3.6% of the assayed gold would be lost.

B. IMPLICATIONS TO ROASTING

- **Submicroscopic Au in arsenopyrite** accounts for the bulk of the assayed gold in the roaster feed (> 90%). **Native Au enclosed in arsenopyrite** is approximately: 3%
- The **submicroscopic Au** in the arsenopyrite is most probably in solid solution, and is **inhomogeneously distributed**
- The **areas with high Au concentrations** (> 1000 ppm) are located in **the outer zone** of the arsenopyrite grains.

- Some calcine particles have a **sintered outer layer** which significantly **reduced permeability** and **'locks' colloidal** gold
- Gold is lost in the calcine residue in the following forms:
  - (i) within mostly impermeable maghemite particles (regrind will have little effect)
  - (ii) in the permeable core of goethite/scorodite particles with sintered coatings (regrind will improve recovery)
  - (iii) in the sintered coating (regrind will have little effect)
- Results indicated that the **gold recovery improves by regrinding** of permeable particles that have sintered coatings
- Pyrite contributes a maximum of 6.4% of the gold in the roaster feed

C. IMPLICATIONS TO CURRENT TAILINGS RECLAIM

- Gold in the current tailings and calcine residue is in the following forms:
  - (i) native Au combined with quartz,
  - (ii) submicroscopic and native Au with fine-grained arsenopyrite,
  - (iii) colloidal Au in maghemite particles,
  - (iv) colloidal Au in more permeable calcine particles,
  - (v) colloidal Au in sintered rims of calcine particles, and

(vi) soluble Au salts??

- Regrinding followed by CIL cyanidation will result in the recovery of (i), (vi) and part of (ii) and (iv).

## 6.0 ACKNOWLEDGEMENTS

The following personnel of Surface Science Western are thanked for contributing to this study: Dr. N.J. Cook (optical microscopy and EDX analysis of native Au), Ms. U. Agha (optical microscopy of sulphides and SEM imaging), Mr. C. Weisener (ion probe microanalysis and imaging), and Mrs. S. Brown for typing the report.

## 7.0 LIST OF REFERENCES

Chryssoulis, S.L. (1987) Mineralogical balance of silver in the Brunswick concentrates and selected intermediate mill products. RPC report MDP/87/18 47 p.

Chryssoulis, S.L. (1989) Quantitative trace precious metal analysis of sulphide and sulpharsenide minerals by SIMS. SIMS VII International conference Proceedings, Wiley and Sons.

Chryssoulis, S.L. and N.J. Cook (1990) Concentrations of 'invisible gold' in common sulphides. Canadian Mineralogist, March issue (in press).

Chryssoulis, S.L. and C.G. Weisener (1989) Precious metal distribution in the Bacubirito iron meteorite by SIMS. SIMS VII International conference Proceedings, Wiley and Sons.

Chryssoulis, S.L., L.J. Cabri and R.S. Salter (1987) Direct determination of invisible gold in refractory sulphide ores in International symposium on Gold Metallurgy, Winnipeg, Pergamon Press, CIM, vol.1., 235-244.

Chryssoulis, S.L., L.J. Cabri and W. Lennard (1989) Calibration of the ion microprobe for quantitative trace precious metal analyses of ore minerals. Econ. Geology, V84, n6 (in press)

Graham, J., J. Just and G. Nyuyen (1988) Electron beam techniques in gold mineralogy, exploration and processing. Perth Gold 88, 137-140.

# APPENDIX A1

## SIZE AND DENSITY ANALYSIS

RESULTS OF SIEVE AND HEAVY LIQUID SEPARATION

| SAMPLE | % + 200 | | | % - 200 cones 1-3 | | % Slimes cones 4,5,dis. |
|---|---|---|---|---|---|---|
| **#1** | 43.0 | | | 20.0 | | 37.0 |
| Classifier o/f | **sink** | **int.** | **float** | **sink** | **float** | |
| as is | 5.7 | 16.9 | 77.4 | 8.2 | 91.8 | |
| **#5** | | (47.8) | | | | 52.2 |
| Classifier o/f -200 Cyan. res. | | | | | | |
| **#8** | 32.3 | | | 24.5 | | 43.2 |
| High grade tails | **sink** | | **float** | **sink** | **float** | |
| as is | 6.3 | | 93.7 | 13.4 | 86.6 | |
| **#11** | 30.7 | | | 26.2 | | 43.1 |
| Low grade tails | **sink** | | **float** | **sink** | **float** | |
| as is | 9.1 | | 90.9 | 13.4 | 86.6 | |
| **#14** Roaster calcine | 29.8 | | | 41.7 | | 28.5 |
| **#15** Calcine residue | 27.5 | | | 44.7 | | 27.8 |
| **#16** Calcine, pulverised & cyanided | 11.3 | | | 38.6 | | 50.1 |
| **#18** 1st Maxwell conc. | 37.9 | | | 41.2 | | 20.9 |
| **#19** 2nd Maxwell conc. | 47.6 | | | 33.9 | | 18.5 |
| **#20** Rougher conc. | 49.7 | | | 27.9 | | 22.4 |
| **#21** Scavenger conc. | 45.9 | | | 16.1 | | 38.0 |

## Procedure

Eleven samples were submitted to be processed on a cyclosizer. Each sample was cut to generate two sub-samples of approximately 50 grams (see Table 1 for sample weights)

The 50 gram sample was weighed to the second decimal, slurried in water and a pinch of sodium meta-phosphate was added as a dispersant. The sample was then introduced in the cylcosizer and left for an elutriation time of 20 minutes (see Table 2 for operating conditions).

As soon as some of the material was exiting cone 5 a sample of the minus cone 5 material was taken for exactly 1 minute. This procedure was repeated for every 50 grams sub-sample.

Table 3 contains the corrected cut-size for every run except for the correction factor for density which is left to you. You will find a graph with the pertaining data to evaluate this factor.

Table 4 and 5 report the weights of each cone fraction for every sample as well as the % weight distribution.

As was mentioned on the phone sample #5 had not been screened at 200 mesh and therefore minor losses occured when retrieving the cone 1 fraction.

Table 1

| Sample # | Cumulative Starting Weight in Grams |
|---|---|
| 1 | 100.65 |
| 5 | 100.79 |
| 8 | 101.27 |
| 11 | 100.60 |
| 14 | 102.28 |
| 15 | 100.37 |
| 16 | 100.68 |
| 18 | 100.46 |
| 19 | 100.77 |
| 20 | 100.47 |
| 21 | 101.37 |

## Table 2

Operating Condition

| Sample # | | |
|---|---|---|
| 1 and 5 | Temperature = 20°C | Correction factor 1.0025 |
| | Elutriation time = 20 minutes | Correction factor 0.955 |
| | Flowrate = Rotameter reading 180 | Correction factor 1.00 |
| | Density = | |
| 8 and 11 | Temperature = 20.25°C | Correction factor 0.9975 |
| | Elutriation time = 20 minutes | Correction factor 0.955 |
| | Flowrate = Rotameter reading 180 | Correction factor 1.00 |
| | Density = | |
| 14, 15, 16, 18, 19, 20 and 21 | Temperature = 19.5 °C | Correction factor 1.0075 |
| | Elutriation time = 20 minutes | Correction factor 0.955 |
| | Flowrate = Rotameter reading 180 | Correction factor 1.00 |
| | Density = | |

## Table 3

Corrected Cut Size in $\mu m^*$

| Sample # | Cone 1 | 2 | 3 | 4 | 5 | -5 |
|---|---|---|---|---|---|---|
| 1 and 5 | 50.74 | 31.40 | 21.92 | 14.74 | 10.72 | -10.72 |
| 8 and 11 | 50.49 | 31.25 | 21.81 | 14.67 | 10.67 | -10.67 |
| All other samples | 50.99 | 31.56 | 22.03 | 14.82 | 10.78 | -10.78 |

* Includes corrections for temperature, flowrate and elutriation time. Excludes correction for density.

## Table 5

% Weight

| Sample # | Cone 1 | 2 | 3 | 4 | 5 | -5 |
|---|---|---|---|---|---|---|
| 1 | 12.53 | 11.03 | 11.47 | 11.57 | 9.63 | 43.78 |
| 5 | 18.84 | 19.59 | 9.38 | 9.23 | 7.50 | 35.47 |
| 8 | 11.95 | 11.86 | 12.17 | 11.88 | 9.59 | 42.56 |
| 11 | 12.60 | 12.51 | 12.64 | 11.92 | 9.33 | 40.98 |
| 14 | 12.12 | 30.94 | 16.29 | 12.32 | 7.57 | 20.76 |
| 15 | 13.19 | 32.33 | 16.10 | 12.22 | 7.34 | 18.81 |
| 16 | 17.29 | 13.67 | 12.61 | 11.21 | 8.28 | 36.93 |
| 18 | 23.94 | 31.35 | 11.07 | 8.33 | 5.50 | 19.81 |
| 19 | 22.20 | 29.99 | 12.44 | 9.62 | 6.24 | 19.51 |
| 20 | 17.28 | 26.32 | 11.80 | 9.72 | 6.84 | 28.04 |
| 21 | 13.01 | 8.47 | 8.19 | 8.87 | 8.40 | 53.05 |

## Table 4

Weight in grams

| Sample # | Cone 1 | 2 | 3 | 4 | 5 | -5 |
|---|---|---|---|---|---|---|
| 1 | 12.61 | 11.10 | 11.54 | 11.65 | 9.69 | 33.34 |
| 5 | 18.99 | 19.74 | 9.45 | 9.30 | 7.56 | 24.80 |
| 8 | 12.10 | 12.01 | 12.32 | 12.03 | 9.71 | 31.71 |
| 11 | 12.68 | 12.59 | 12.72 | 11.99 | 9.39 | 30.40 |
| 14 | 12.40 | 31.65 | 16.66 | 12.60 | 7.74 | 10.76 |
| 15 | 13.24 | 32.45 | 16.16 | 12.27 | 7.37 | 10.85 |
| 16 | 17.41 | 13.76 | 12.70 | 11.29 | 8.34 | 21.04 |
| 18 | 24.05 | 31.49 | 11.12 | 8.37 | 5.53 | 12.65 |
| 19 | 22.37 | 30.22 | 12.54 | 9.69 | 6.29 | 11.10 |
| 20 | 17.36 | 26.44 | 11.86 | 9.77 | 6.87 | 19.02 |
| 21 | 13.19 | 8.59 | 8.30 | 8.99 | 8.52 | 40.42 |

# APPENDIX A2

## CHEMICAL ASSAYS

## GIANT YELLOWKNIFE

## LAKEFIELD RESEARCH

LAKEFIELD RESEARCH
A DIVISION OF FALCONBRIDGE LIMITED
P.O. Box 430, 185 Concession St., LAKEFIELD, ON K0L 2H0
Phone: (705) 652-3341, Facsimile: (705) 652-6365, Telex: 0696-2842

No.: 7662

# CERTIFICATE OF ANALYSIS

University of Western Ontario
Natural Sciences Centre, Room 6
London, Ontario N6A 5B7
Att: Dr. S.L. Chryssoulis - Confidential

Date: July 17, 1989
Sample Received: July 10, 1989
No. of Samples: 30
Our Reference No.: 3932316
Your P.O. No.:

Samples submitted to us show results as follows:

| Sample No. | | As % | S % | Au g/t |
|---|---|---|---|---|
| Head | 1 | 0.92 | 2.03 | 8.64 |
| [illegible] | 2 | 7.06 | 25.3 | 87.2 |
| [illegible] | 3 | DID NOT | RECEIVE | SAMPLE #3 |
| [illegible] | 4 | 0.093 | 0.12 | 1.07 |
| [illegible] | 5 | 0.52 | 0.80 | 3.42 |
| [illegible] | 6 | 1.10 | 1.98 | 10.1 |
| [illegible] | 7 | 0.85 | 2.06 | 5.45 |
| [illegible] | 8 | 0.086 | 0.16 | 0.81 |
| [illegible] | 9 | 0.48 | 1.03 | 8.51 |
| [illegible] | 10 | 0.20 | 0.50 | 1.71 |
| [illegible] | 11 | 0.062 | 0.05 | 0.21 |
| [illegible] | 12 | 0.061 | 0.09 | 0.20 |
| [illegible] | 13 | 0.080 | 0.14 | 0.71 |
| [illegible] | 14 | 0.081 | 0.16 | 0.21 |
| [illegible] | 15 | 0.25 | 0.46 | 1.34 |
| [illegible] | 16 | 0.20 | 0.65 | 1.70 |
| [illegible] | 17 | 0.038 | 0.05 | 0.25 |
| [illegible] | 18 | 0.049 | 0.07 | 0.08 |
| [illegible] | 19 | 0.073 | 0.12 | 0.13 |
| [illegible] | 20 | 1.69 | 3.52 | 91.7 |
| [illegible] | 21 | 1.60 | 3.43 | 4.52 |
| [illegible] | 22 | 1.78 | 3.45 | 6.33 |
| [illegible] | 23 | 1.64 | 3.48 | 91.4 |
| [illegible] | 24 | 1.59 | 3.41 | 4.58 |
| [illegible] | 25 | 1.73 | 3.42 | 6.38 |
| [illegible] | 26 | 12.7 | 32.1 | 110. |
| [illegible] | 27 | 12.2 | 37.0 | 117. |
| [illegible] | 28 | 10.1 | 16.1 | 82.2 |
| [illegible] | 29 | 3.00 | 3.94 | 28.4 |
| | 30 | 35.2 | 14.5 | 69.2 |

91.1
3.77, 4.11

Additional Copies to

Signed: J.R. Hunter
A.E. Carr, Manager - Assay Services

NOTE: Rejects will be discarded after 6 months
Please, inquire about our long-term storage facilities

RESULTS OF CHEMICAL ASSAYS

| SAMPLE | unseparated | | | +200 sink | | | -200 float cones 1-3 | | | Slimes cones 4,5,dis | | |
|---|---|---|---|---|---|---|---|---|---|---|---|---|
| | As% | S% | Au | As% | S% | Au | As% | S% | Au | As% | S% | Au |
| #1 Classifier o/f as is | 1.01 ±.18 | 2.01 ±.05 | 9.37 ±1.46 | 7.06 | 25.3 | 87.2 | 0.09 | 0.12 | 1.07 | 0.52 | 0.80 | 3.42 |
| #5 Classifier o/f -200 Cyan. res. | 0.85 | 2.06 | 5.45 | - | - | - | - | - | - | - | - | - |
| #8 High grade tails as is | 0.08 ±.01 | 0.15 ±.02 | 0.76 ±.10 | 0.48 | 1.03 | 8.51 | 0.06 | 0.05 | 0.21 | 0.06 | 0.09 | 0.20 |
| | (-200 sink: | | | 0.20 | 0.50 | 1.71) | | | | | | |
| #11 Low grade tails as is | 0.08 ±.01 | 0.14 ±.04 | 0.17 ±.08 | 0.25 | 0.46 | 1.34 | 0.04 | 0.05 | 0.25 | 0.05 | 0.07 | 0.08 |
| | (-200 sink: | | | 0.20 | 0.65 | 1.70) | | | | | | |

| | Unseparated sample | | |
|---|---|---|---|
| | As % | S % | Au (g/t) |
| #14 Roaster calcine | 1.67 ±.05 | 3.50 ±.04 | 91.5 ±0.3 |
| #15 Calcine residue | 1.75 ±.05 | 3.43 ±.03 | 6.35 ±.05 |
| #16 Calcine, pulverised & cyanided | 1.60 ±.01 | 3.42 ±.02 | 4.55 ±.06 |
| #18 1st Maxwell conc. | 12.7 | 32.1 | 110. |
| #19 2nd Maxwell conc. | 12.2 | 37.0 | 117. |
| #20 Rougher conc. | 10.1 | 16.1 | 82.2 |
| #21 Scavenger conc. | 3.0 | 3.94 | 28.4 |

Flotation Concentrates.

| | Au | Fe | S | As | Weight |
|---|---|---|---|---|---|
| 1st Maxwell Cell | 3.17 | 27.5 | 27.48 | 11.04 | 735 |
| 2cond Maxwell Cell | 3.21 | 34.25 | 31.98 | 10.73 | 512 |
| Rougher Conc. | 2.38 | 18.75 | 15.27 | 8.79 | 400 |
| Scavenger Conc. | .75 | 8.25 | 5.37 | 3.04 | 233 |
| | | | | | 1.88k |
| | | | | Total weight | 18.141 |

| Results: | Marking Code | oz/T Au | Fe | S | As | Sb | Weight |
|---|---|---|---|---|---|---|---|
| ) Classifier O/F | | | | | | | |
| Head sample | 1 | .125 | 7.25 | 2.2 | | .88 | 813 |
| 200 Mesh (as is) | 2 | .125 | 7.25 | 2.04 | | .89 | 631 |
| 275 Mesh " | 3 | .125 | 7.175 | 2.53 | | .88 | 643 |
| 325 Mesh " | 4 | .125 | 7.25 | 2.49 | | .88 | 643 |
| anided -200 Mesh | 5 | .153 | 7.175 | 1.89 | | .79 | 479 |
| -275 Mesh | 6 | .154 | 7.0 | 1.99 | | .84 | 475 |
| -325 Mesh | 7 | .151 | 5.75 | 2.02 | | .85 | 475 |
| | | | | | | subtotal | 4.18 |
| Flotation Tails | | | | | | | |
| High assayed flot tails | | | | | | | |
| head sample | 8 | .019 | – | .25 | | – | 913 |
| +pulverized but cyanided | 9 | .010 | 5.00 | .24 | | .02 | 448 |
| pulverized + cyanided | 10 | .010 | 5.25 | .23 | | .02 | 495 |
| | | | | | | subtotal | 1.85 |
| low assayed flot tails | | | | | | | |
| head sample | 11 | .014 | – | .27 | | .03 | 24 |
| pulverized but cyanided | 12 | .007 | – | .15 | | .06 | 447 |
| pulverized + cyanided | 13 | .007 | – | .15 | | .06 | 477 |
| | | 0.325 | | | | subtotal | 1.16 |
| Roaster Calcine | | Au | Fe | S | As | Sb | |
| head sample | 14 | 2.69 | 31.25 | 3.9 | 1.40 | .38 | 5.9 |
| Cyanided as is (calcine residue) | 15 | .012 | 28.5 | 4.0 | 1.30 | " | 2.2 |
| Pulverized, then cyanided | 16 | " | " | " | " | | 486 |
| cyanided, pulverized, cyanided | 17 | .013 | | | | | 489 |
| | | | | | | subtotal | 9.074 |

# APPENDIX A3

## RESULTS OF OPTICAL MICROSCOPY ON NATIVE Au

#1 Classifier o/f

Native gold grains in +200 mesh sink fraction

Enclosed in Pyrite

| Grain | Size (μm²) | Au% | Grain | Size (μm²) | Au% |
|---|---|---|---|---|---|
| 1 | 60 | 84.9 | 26 | 22 | 99.7 |
| 2 | 40 | 89.3 | 27 | 60 | 93.2 |
| 3 | 9 | 91.2 | 28 | 5 | 91.3 |
| 4 | 4 | 98.5 | 29 | 600 | 95.0 |
| 5 | 12 | 96.4 | 30 | 1 | - |
| 6 | 135 | 97.7 | 31 | 4 | - |
| 7 | 12 | - | 32 | 3 | - |
| 8 | 1 | - | 33 | 3 | - |
| 9 | 40 | - | 34 | 7 | - |
| 10 | 7 | - | 35 | 9 | 96.3 |
| 11 | 14 | 98.6 | 36 | 2 | - |
| 12 | 1 | - | 37 | 3 | - |
| 13 | 3 | - | 38 | 15 | 96.1 |
| 14 | 145 | 98.2 | 39 | 120 | 89.2 |
| 15 | 5 | - | 40 | 12 | 97.3 |
| 16 | 25 | 94.4 | 41 | 6 | - |
| 17 | 17 | 97.7 | 42 | 60 | 93.1 |
| 18 | 25 | 88.8 | 43 | 10 | - |
| 19 | 7 | - | 44 | 120 | 93.4 |
| 20 | 13 | 96.5 | 45 | 1 | - |
| 21 | 9 | 96.9 | 46 | 115 | 94.0 |
| 22 | 5 | 97.3 | 47 | 1 | - |
| 23 | 5 | - | 48 | 70 | 92.3 |
| 24 | 10 | 98.7 | 49 | 24 | 94.2 |
| 25 | 23 | 98.4 | 50 | 15 | - |

Combined with pyrite

| Grain | Size (μm²) | Au% |
|---|---|---|
| 51 | 350 | 92.8 |
| 52 | 70 | 91.0 |
| 53 | 20 | - |
| 54 | 304 | 87.8 |

**TABLE**

## Enclosed in coarse-grained arsenopyrite

| Grain | Size ($\mu m^2$) | Au% | Grain | Size ($\mu m^2$) | Au% |
|---|---|---|---|---|---|
| 55 | 18 | 80.7 | 69 | 3 | - |
| 56 | 16 | 81.2 | 70 | 13 | 84.2 |
| 57 | 1 | - | 71 | 9 | - |
| 58 | 35 | 80.5 | 72 | 2 | - |
| 59 | 5 | - | 73 | 2 | - |
| 60 | 7 | - | 74 | 1 | - |
| 61 | 20 | 73.8 | 75 | 1 | - |
| 62 | 2 | - | 76 | 25 | 88.0 |
| 63 | 2 | - | 77 | 12 | 91.3 |
| 64 | 7 | 93.4 | 78 | 90 | 92.8 |
| 65 | 150 | 91.1 | 79 | 15 | 94.8 |
| 66 | 4 | - | 80 | 18 | 92.5 |
| 67 | 4 | - | 81 | 48 | 95.4 |
| 68 | 1 | - | 82 | 72 | 93.7 |

## Combined with coarse-grained arsenopyrite

| Grain | Size ($\mu m^2$) | Au% | Grain | Size ($\mu m^2$) | Au% |
|---|---|---|---|---|---|
| 83 | 4 | - | 92 | 100 | 86.7 |
| 84 | 125 | 88.5 | 93 | 15 | 93.9 |
| 85 | 320 | 87.4 | 94 | 9 | 79.6 |
| 86 | 110 | 87.2 | 95 | 5 | 91.7 |
| 87 | 2 | - | 96 | 4 | - |
| 88 | 20 | - | 97 | 2 | - |
| 89 | 16 | 75.1 | 98 | 36 | - |
| 90 | 5 | 73.8 | 99 | 5 | - |
| 91 | 60 | 75.7 | 100 | 5 | 87.5 |

**TABLE**

**Enclosed in fine-grained arsenopyrite**

| Grain | Size (μm²) | Au% |
|---|---|---|
| 101 | 3 | - |
| 102 | 4 | - |
| 103 | 45 | 93.3 |
| 104 | 28 | 92.6 |
| 105 | 1 | - |
| 106 | 1 | - |
| 107 | 1 | - |
| 108 | 4 | - |
| 109 | 7 | 97.7 |
| 110 | 1 | - |
| 111 | 4 | - |
| 112 | 1 | - |
| 113 | 2 | - |
| 114 | 2 | - |
| 115 | 1 | - |
| 116 | 2 | - |
| 117 | 8 | 90.4 |
| 118 | 16 | 89.0 |
| 119 | 1 | - |
| 120 | 2 | - |
| 121 | 2 | - |
| 122 | 8 | - |
| 123 | 10 | 92.3 |
| 124 | 2 | - |
| 125 | 5 | - |
| 126 | 40 | 83.3 |
| 127 | 35 | - |
| 128 | 150 | 93.4 |
| 129 | 4 | 93.0 |
| 130 | 4 | - |
| 131 | 4 | - |
| 132 | 6 | 90.1 |
| 133 | 125 | 87.1 |
| 134 | 6 | - |
| 135 | 20 | 90.5 |
| 136 | 15 | 89.7 |
| 137 | 3 | - |
| 138 | 7 | 89.1 |
| 139 | 1 | - |
| 140 | 4 | - |
| 141 | 3 | - |
| 142 | 1 | - |
| 143 | 2 | - |
| 144 | 2 | - |
| 145 | 105 | 92.0 |
| 146 | 32 | - |
| 147 | 12 | - |
| 148 | 90 | - |
| 149 | 3 | - |
| 150 | 7 | - |
| 151 | 6 | - |
| 152 | 8 | 87.1 |
| 153 | 4 | - |
| 154 | 1 | - |
| 155 | 1 | - |
| 156 | 6 | - |
| 157 | 1 | - |
| 158 | 2 | - |
| 159 | 9 | - |
| 160 | 17 | 98.3 |
| 161 | 15 | - |
| 162 | 7 | - |
| 163 | 50 | 92.8 |
| 164 | 60 | 84.5 |
| 165 | 4 | - |
| 166 | 2 | - |
| 167 | 25 | 100.0 |
| 168 | 35 | 99.7 |
| 169 | 1 | - |
| 170 | 15 | - |
| 171 | 4 | - |
| 172 | 20 | 99.4 |
| 173 | 10 | 99.3 |
| 174 | 205 | 89.1 |
| 175 | 4 | 99.8 |
| 176 | 2 | 99.7 |
| 177 | 6 | 99.3 |
| 178 | 22 | 98.9 |
| 179 | 40 | 98.6 |
| 180 | 150 | 99.0 |
| 181 | 7 | 92.1 |
| 182 | 43 | 91.3 |
| 183 | 140 | 87.6 |
| 184 | 5 | 90.6 |
| 185 | 20 | 89.8 |
| 186 | 5 | 92.0 |
| 187 | 278 | 90.4 |
| 188 | 55 | 88.8 |
| 189 | 1 | - |

**TABLE**

| Liberated | | | Enclosed in Fe-oxide | | |
|---|---|---|---|---|---|
| Grain | Size ($\mu m^2$) | Au% | Grain | Size ($\mu m^2$) | Au% |
| 190 | 500 | 91.2 | 196 } | 6 | - |
| 191 | 90 | - | 197 } | 2 | - |
| 192 | 120 | 89.0 | 198 | 6 | 90.1 |
| 193 | 1600 | 82.0 | | | |
| 194 | 7500 | 91.1 | | | |
| 195 | 8848 | 90.3 | | | |

#1 Classifier o/f

**Native gold grains in +200 mesh intermediate fraction**

| Grain | Size ($\mu m^2$) | Au% |
|---|---|---|
| Enclosed in fine-grained arsenopyrite-quartz particle | | |
| 1 | 18 | 91.3 |
| 2 | 21 | 90.1 |
| 3 | 75 | - |
| 4 | 24 | - |
| 5 | 35 | 81.2 |
| 6 | 9 | 99.8 |
| 7 | 8 | 99.2 |
| 8 | 3 | - |
| TOTAL | 193 | |

193 × 4.7 = 907 $\mu m^2$

## #1 Classifier o/f -200 mesh sink fraction

### Native gold grains

**Combined with pyrite**

| Grain | Size (μm²) |
|---|---|
| 1 | 1 |
| 2 | 378 |

**Combined with f-g aspy**

| Grain | Size (μm²) |
|---|---|
| 8 | 168 |
| 9 | 6 |

**Enclosed in c-g aspy**

| Grain | Size (μm²) |
|---|---|
| 3 | 4 |

**Liberated**

| Grain | Size (μm²) |
|---|---|
| 10 | 1218 |
| 11 | 134 |
| 12 | 87 |
| 13 | 94 |
| 14 | 704 |
| 15 | 82 |
| | 2,319 |

**Combined with c-g aspy**

| Grain | Size (μm²) |
|---|---|
| 4 | 38 |
| 5 | 5 |
| 6 | 21 |
| 7 | 139 |

#8 High grade tailings +200 mesh sink fraction

Native gold grains

Enclosed in fine-grained arsenopyrite

| Grain | Size (μm²) | Au % |
|---|---|---|
| 1 | 22 | - |
| 2 | 8 | - |

Combined with quartz

| | | |
|---|---|---|
| 3 | 600 | 92.6 |
| 4 | 520 | 93.9 |
| 5 | 17 | - |

#11 low grade tailings +200 mesh sink fraction

Native gold grains

Enclosed in fine-grained arsenopyrite

| Grain | Size (μm²) |
|---|---|
| 1 | 11 |
| 2 | 8 |
| 3 | 18 |

#8 High grade tailings -200 mesh sink fraction

Native gold grains

Enclosed in quartz

| Grain | Size (μm²) |
|---|---|
| 1 | 459 |

#11 low grade tailings -200 mesh sink fraction

Native gold grains

.....none.....

## #18 1st Maxwell Concentrate +200 mesh fraction

### Native gold grains

**Enclosed in pyrite**

| Grain | Size (µm²) |
|---|---|
| 1 | 5 |
| 2 | 32 |
| 3 | 147 |
| 4 | 82 |
| 5 | 46 |
| 6 | 48 |
| | 360 |

**Enclosed in stibnite**

| Grain | Size (µm²) |
|---|---|
| 33 | 1 |
| 34 | 1 |
| 35 | 3 |
| 36 | 3 |
| 37 | 2 |
| 38 | 3 |
| 39 | 4 |
| 40 | 1 |
| | 18 |

**Combined with pyrite**

| Grain | Size (µm²) |
|---|---|
| 7 | 57 |
| 8 | 49 |
| | 106 |

**Enclosed in c-g aspy**

| Grain | Size (µm²) |
|---|---|
| 9 | 2 |
| 10 | 2 |
| 11 | 105 |
| 12 | 26 |
| 13 | 1 |
| 14 | 2 |
| 15 | 15 |
| 16 | 143 |
| 17 | 8 |
| 18 | 16 |
| 19 | 4 |
| 20 | 7 |
| 21 | 10 |
| 22 | 5 |
| 23 | 11 |
| 24 | 23 |
| 25 | 26 |
| 26 | 35 |
| 27 | 1 |
| 28 | 22 |
| 29 | 12 |
| 30 | 3 |
| 31 | 50 |
| 32 | 37 |
| | 561 |

**Liberated**

| Grain | Size (µm²) | % Au |
|---|---|---|
| 41 | 13248 | 93.7 |

4.1% of the visible Au area is finer than 300µm² and locked.

# #18 1st Maxwell Concentrate -200 mesh fraction

## Native gold grains

### Enclosed in pyrite

| Grain | Size (μm²) |
|---|---|
| 1 | 8 |
| 2 | 97 |
| 3 | 13 |
| 4 | 10 |
| 5 | 7 |
| 6 | 6 |
| 7 | 17 |
| 8 | 15 |
| 9 | 3 |
| | 176 |

### Combined with pyrite

| Grain | Size (μm²) |
|---|---|
| 10 | 62 |
| 11 | 5 |
| 12 | 59 |
| 13 | 88 |
| 14 | 5 |
| 15 | 7 |
| 16 | 9 |
| | 235 |

### Enclosed in c-g aspy

| Grain | Size (μm²) |
|---|---|
| 17 | 14 |
| 18 | 16 |
| 19 | 2 |
| 20 | 1 |
| 21 | 4 |
| 22 | 4 |
| 23 | 7 |
| 24 | 120 |
| 25 | 4 |
| | 172 |

### Combined with c-g aspy

| Grain | Size (μm²) |
|---|---|
| 26 | 537 |
| 27 | 1020 |
| 28 | 5 |
| 29 | 1105 |
| 30 | 38 |
| 31 | 36 |
| 32 | 173 |
| 33 | 18 |
| | 2932 |

### Liberated

| Grain | Size (μm²) |
|---|---|
| 34 | 762 |
| 35 | 416 |
| 36 | 46 |
| 37 | 147 |
| 38 | 155 |
| 39 | 20 |
| 40 | 43 |
| 41 | 50 |
| 42 | 162 |
| 43 | 28 |
| 44 | 83 |
| 45 | 75 |
| 46 | 96 |
| 47 | 74 |
| 48 | 43 |
| 49 | 60 |
| 50 | 37 |
| 51 | 31 |
| 52 | 45 |
| 53 | 57 |
| 54 | 72 |
| 55 | 59 |
| 56 | 22 |
| | 2583 |

5.7% of the native Au is finer than 300 μm² and is locked

## #19 2nd Maxwell Concentrate +200 mesh fraction

### Native gold grains

**Enclosed in pyrite**

| Grain | Size (μm²) |
|---|---|
| 1 | 9 |
| 2 | 1 |
| 3 | 2 |
| 4 | 1 |
| 5 | 1 |
| 6 | 4 |
| 7 | 19 |
| 8 | 21 |
| 9 | 3 |
| 10 | 72 |
| 11 | 81 |
| 12 | 5 |
| 13 | 2 |
| 14 | 1 |
| 15 | 5 |
| 16 | 19 |
| 17 | 9 |
| 18 | 10 |
| 19 | 15 |
| 20 | 14 |
| 21 | 2 |
| 22 | 3 |
| | 299 |

**Enclosed in f-g arsenopyrite**

| Grain | Size (μm²) |
|---|---|
| 33 | 25 |
| 34 | 44 |
| 35 | 21 |
| 36 | 28 |
| 37 | 62 |
| 38 | 135 |
| 39 | 6 |
| 40 | 4 |
| 41 | 4 |
| 42 | 29 |
| 43 | 62 |
| 44 | 11 |
| 45 | 35 |
| | 460 |

**Combined with pyrite**

| Grain | Size (μm²) |
|---|---|
| 23 | 32 |
| 24 | 247 |
| 25 | 85 |
| 26 | 4 |
| 27 | 231 |
| 28 | 19 |
| 29 | 544 |
| 30 | 13 |
| 31 | 7 |
| 32 | 11 |
| | 1193 |

**Liberated**

| Grain | Size (μm²) | Au % |
|---|---|---|
| 46 | 44820 | 91.6 |
| 47 | 4800 | 92.7 |
| 48 | 650 | 92.2 |

1.5% of the native Au is locked and finer than 300 μm².

# #19 2nd Maxwell Concentrate -200 mesh fraction

## Native gold grains

### Enclosed in pyrite

| Grain | Size (μm²) |
|---|---|
| 1 | 78. |

### Combined with pyrite

| Grain | Size (μm²) |
|---|---|
| 2 | 126 |
| 3 | 66 |
| | 192 |

### Combined with c-g aspy

| Grain | Size (μm²) |
|---|---|
| 4 | 12 |
| 5 | 19 |
| 6 | 24 |
| 7 | 37 |
| | 92 |

### Enclosed in acanthite

| Grain | Size (μm²) |
|---|---|
| 8 | 13 |
| 9 | 11 |
| 10 | 2 |
| 11 | 3 |
| 12 | 2 |
| 13 | 4 |
| 14 | 24 |
| 15 | 6 |
| 16 | 5 |
| 17 | 9 |
| 18 | 3 |
| 19 | 5 |
| 20 | 3 |
| | 90 |

### Liberated

| Grain | Size (μm²) |
|---|---|
| 21 | 76 |
| 22 | 144 |
| 23 | 18 |
| 24 | 15 |
| 25 | 131 |
| 26 | 126 |
| 27 | 74 |
| 28 | 59 |
| 29 | 32 |
| 30 | 114 |
| 31 | 123 |
| 32 | 95 |
| 33 | 512 |
| 34 | 768 |
| 35 | 93 |
| 36 | 29 |
| 37 | 48 |
| 38 | 77 |
| 39 | 44 |
| | 2577 |

### Combined with acan

| Grain | Size (μm²) |
|---|---|
| 40 | 84 |
| 41 | 37 |
| 42 | 132 |
| 43 | 141 |
| 44 | 16 |
| | 410 |

4.9% of the native Au is locked and finer than 300 μm².

## #20 Rougher Concentrate +200 mesh fraction

### Native gold grains

**Enclosed in pyrite**

| Grain | Size (μm²) |
|---|---|
| 1 | 9 |

**Combined with pyrite**

| Grain | Size (μm²) |
|---|---|
| 2 | 323 |

**Combined with f-g aspy**

| Grain | Size (μm²) |
|---|---|
| 14 | 23 |
| 15 | 2 |
| 16 | 31 |
| 17 | 19 |
| 18 | 3 |
| 19 | 2 |
| 20 | 18 |
| 21 | 197 |
| | 295 |

**Enclosed in f-g aspy**

| Grain | Size (μm²) |
|---|---|
| 3 | 4 |
| 4 | 5 |
| 5 | 1 |
| 6 | 1 |
| 7 | 1 |
| 8 | 3 |
| 9 | 2 |
| 10 | 3 |
| 11 | 3 |
| 12 | 11 |
| 13 | 10 |
| | 44 |

**Combined with pyrrhotite**

| Grain | Size (μm²) |
|---|---|
| 22 | 154 |

**Liberated**

| Grain | Size (μm²) |
|---|---|
| 23 | 35 |
| 24 | 140 |
| 25 | 2176 |
| | 2351 |

## #21 Scavenger Concentrate +200 mesh fraction

### Native gold grains

**Combined with f-g aspy**

| Grain | Size (μm²) |
|---|---|
| 1 | 71 |
| 2 | 23 |
| 3 | 9 |
| 4 | 35 |
| 5 | 26 |
| 6 | 17 |

## #20 Rougher Concentrate -200 mesh fraction

### Native gold grains

| Combined with f-g aspy | | Liberated | |
|---|---|---|---|
| Grain | Size (μm²) | Grain | Size (μm²) |
| 1 | 13 | 12 | 164 |
| 2 | 6 | 13 | 272 |
| 3 | 11 | 14 | 432 |
| 4 | 14 | 15 | 71 |
| 5 | 3 | 16 | 491 |
| 6 | 3 | 17 | 512 |
| 7 | 7 | 18 | 958 |
| 8 | 10 | 19 | 157 |
| 9 | 14 | 20 | 26 |
| 10 | 7 | 21 | 37 |
| 11 | 12 | 22 | 101 |
| | | 23 | 28 |
| | | 24 | 17 |
| | | 25 | 37 |
| | | 26 | 74 |
| | | 27 | 17 |
| | | 28 | 79 |
| | | 29 | 67 |

## #21 Scavenger Concentrate -200 mesh fraction

### Native gold grains

**Combined with f-g aspy**

| Grain | Size (μm²) |
|---|---|
| 1 | 8 |
| 2 | 29 |
| 3 | 3 |
| 4 | 39 |
| 5 | 1 |
| 6 | 3 |
| 7 | 6 |
| 8 | 3 |

Statistical Summary

#1 Classifier o/f +200 mesh sink fraction

| | | n | % of Σn | Σarea | % of Σarea |
|---|---|---|---|---|---|
| Grains | < 5 μm² | 80 | 40.4 | 216 | 0.9 |
| Grains | 5- 20 μm² | 59 | 29.8 | 679 | 2.7 |
| Grains | 20- 60 μm² | 28 | 14.2 | 1093 | 4.4 |
| Grains | 60-150 μm² | 21 | 10.6 | 2392 | 9.6 |
| Grains | 150-600 μm² | 7 | 3.5 | 2557 | 10.3 |
| Grains | > 600 μm² | 3 | 1.5 | 17948 | 72.1 |
| | Total | 198 | 100.0 | 24885 | 100.0 |

**#1 Classifier o/f +200 mesh sink fraction**

Enclosed gold grains < 60 $\mu m^2$

| | n | Σarea | % of all gold |
|---|---|---|---|
| Enclosed in pyrite | 43 | 611 | 2.4 |
| Enclosed in c-g arsenopyrite | 25 | 271 | 1.1 |
| Enclosed in f-g arsenopyrite | 81 | 885 | 3.6 |
| Enclosed in Fe-oxide | 3 | 15 | 0.1 |
| Total | 152 | 1782 | 7.2 |
| Fraction of all native gold grains | 76.8% | 7.2% | - |

Statistical Summary

#1 Classifier o/f +200 mesh sink fraction

| | n | Σarea | x area | % |
|---|---|---|---|---|
| Enclosed in pyrite | 50 | 1915 | 38 | 7.7 |
| Combined with pyrite | 4 | 744 | 186 | 3.0 |
| Total | 54 | 2659 | 49 | 10.7 |
| Enclosed in c-g aspy | 28 | 583 | 21 | 2.3 |
| Combined with c-g aspy | 18 | 843 | 47 | 3.4 |
| Total | 46 | 1426 | 31 | 5.7 |
| Enclosed in f-g aspy | 89 | 2128 | 24 | 8.6 |
| Liberated | 6 | 18658 | 3109 | 74.9 |
| Enclosed in Fe-oxide | 3 | 14 | 5 | 0.1 |
| **GRAND TOTAL** | **198** | **24885** | **126** | **100.0** |

#1 Classifier o/f +200 mesh intermediate fraction

| | | | | |
|---|---|---|---|---|
| Enclosed in f-g aspy | 8 | 188 | 24 | 100.0 |
| **GRAND TOTAL** | **8** | **188** | **24** | **100.0** |

## APPENDIX A4 - CORRECTION FACTORS FOR ESTIMATING THE PERCENTAGE OF THE TYPES OF NATIVE AU ASSOCIATIONS

| Size Fractions | +200 | | | 1-3 cones | | 4-5 cones + discharge |
|---|---|---|---|---|---|---|
| wt% | 43 | | | 20 | | 37 |
| Density Fractions | Sink | Inter. | Float | Sink | Float | unseparated |
| wt% | 3.9 | 11.4 | 52.7 | 2.6 | 29.4 | - |
| Sections Studies | 8 | 5 | - | 5 | - | - |
| Correction Factor | x1.0 | x4.7 | - | x1.07 | - | - |
| %Au associated[1] with quartz | | | 1.8 | | 1.6 | |

[1]The Au associated with quartz was calculated from the 1-3 cones float fraction assay by subtracting the Au in the submicroscopic Au in the arsenopyrite.

## APPENDIX A6 - CALCULATION OF DISTRIBUTION OF SUBMISCROPIC GOLD

### SUBMICROSCOPIC Au CONCENTRATION (ppm)

| | n[1] | $\hat{x}$[2] | ±: | λ[3] | | MIN | MAX |
|---|---|---|---|---|---|---|---|
| ARSENOPYRITE | 105 | 299. | | 101. | (34%) | 0.56 | 2,900. |
| coarse | 68 | 153. | | 90. | (59%) | 0.56 | 1,200. |
| fine | 37 | 495. | | 164. | (33%) | 4.0 | 2,900. |
| PYRITE | 96 | 4.7 | | 1.24 | (29%) | 0.34 | 42. |

### Au MINERALOGICAL DISTRIBTUION (g/t)

| | Au assay | NonCN,Au | APY | PY |
|---|---|---|---|---|
| classifier o/f | 8.89 | 5.23±0.06 | 5.65[4] | 0.148 |
| 'high' grade tails | 0.72 | 0.343 | 0.54[4] | 0.015 |
| 'low' grade tails | 0.48 | 0.240 | 0.39[4] | 0.011 |
| 1st Max. cell conc. | 109.3 | 70.0 | 64.4[5] | 2.4 |
| 2nd Max. cell conc. | 113.5 | 72.6 | 57.7[5] | 2.8 |
| Rougher concentrate | 81.9 | 58.1 | 53.3[5] | 1.03 |
| Scavenger concentrate | 27.1 | 20.3 | 22.1[5] | 0.30 |

[1] n: number of particles
[2] $\hat{x}$: average submicroscopic gold concentration
[3] λ: confidence interval of average at 95% significance level
[4] coarse and fine apy
[5] coarse and fine apy by point counting

APPENDIX A5 - TOTAL AREAS ($\mu m^2$) OF NATIVE AU GROUPED ACCORDING TO ASSOCIATION (classifer o/f)

| | | +200 Sink | +200 Int | 1-3 Sink | Comb.Float | % | % |
|---|---|---|---|---|---|---|---|
| Liberated | | 18,658 | - | 2,481 | | 72.7 | 26.1 |
| Py | Encl. | 1,915 | - | - | | 6.6 | 2.4 |
| | Comb. | 744 | - | 406 | | 4.0 | 1.4 |
| c-Apy | Encl. | 583 | - | 4 | | 2.0 | 0.7 |
| | Comb. | 843 | - | 217 | | 3.6 | 1.3 |
| f-Apy | Encl. | 2,128 | - | - | | 7.3 | 2.6 |
| | Comb. | - | - | 186 | | 0.6 | 0.2 |
| Fe ox | Encl. | 14 | - | - | | 0.1 | 0.0 |
| qtz | Assoc. | - | 907 | - | 2.9%[1] | 3.1 | 1.1 |
| | | | | | TOTAL | 100.0 | 35.8 |

[1] calculated from Au assay after subtracting the submicroscopic Au in the arsenopyrite